

**EFFECTS OF BRAN FROM SORGHUM GRAINS CONTAINING DIFFERENT
CLASSES AND LEVELS OF BIOACTIVE COMPOUNDS IN COLON
CARCINOGENESIS**

A Thesis

by

JAYME BETH LEWIS

Submitted to the Office of Graduate Studies of
Texas A&M University
in partial fulfillment of the requirements for the degree of

MASTER OF SCIENCE

December 2008

Major Subject: Nutrition

**EFFECTS OF BRAN FROM SORGHUM GRAINS CONTAINING DIFFERENT
CLASSES AND LEVELS OF BIOACTIVE COMPOUNDS IN COLON
CARCINOGENESIS**

A Thesis

by

JAYME BETH LEWIS

Submitted to the Office of Graduate Studies of
Texas A&M University
in partial fulfillment of the requirements for the degree of

MASTER OF SCIENCE

Approved by:

Chair of Committee,
Committee Members,

Nancy D. Turner
Joanne R. Lupton
Robert S. Chapkin
Lloyd W. Rooney

Chair of Intercollegiate
Faculty of Nutrition,

Stephen B. Smith

December 2008

Major Subject: Nutrition

ABSTRACT

Effects of Bran from Sorghum Grains Containing Different Classes and Levels of Bioactive Compounds in Colon Carcinogenesis. (December 2008)

Jayne Beth Lewis, B.S., Texas A&M University

Chair of Advisory Committee: Dr. Nancy D. Turner

In order to test the dietary effects of bioactive compounds present in whole grains, we decided to observe the effect of varying types of sorghum bran on colon cancer promotion. We used 40 rats consuming diets containing 6% fiber from either cellulose or bran from white (contains phenolic acids), brown (contains tannins), or black (contains anthocyanins) sorghum (n=10). Diets were fed for 10 wk, during which two azoxymethane (AOM) injections (15 mg/kg BW) were administered in wk 3 and 4.

We observed that the total number of aberrant crypts (AC) and high multiplicity aberrant crypt foci (HMACF) were lower in rats consuming black ($p < 0.04$) and brown ($p < 0.006$) sorghum diets when compared to the cellulose diet, and that these decreases were an inverse function of diet antioxidant activity (ABTS). These observations led us to evaluate the effect of these diets on endogenous enzymatic activities (superoxide dismutase, SOD; catalase, CAT; and glutathione peroxidase, GPx), redox status as measured by reduced and oxidized glutathione, and cell cycle processes, proliferation and apoptosis, in the rat colon. Total SOD activity was higher ($p < 0.04$) in rats consuming black sorghum when compared to all other diets. A similar, but not

significant, trend occurred in mitochondrial SOD. The white sorghum diet had enhanced ($p < 0.02$) CAT activity compared to the cellulose diet, but the black and brown sorghum diets were intermediate. Finally, all sorghum diets suppressed GPx activity relative to cellulose ($p < 0.04$). However, no changes were seen in levels of reduced and oxidized glutathione or the ratio of the two.

The black sorghum fed rats had a lower proliferative index ($p < 0.01$) and zone ($p < 0.04$) compared to cellulose; brown and white sorghum rats were intermediate. Apoptotic index was highest in brown sorghum rats compared to cellulose ($p < 0.03$), while other sorghum diets were intermediate. These data suggest that the suppression of AC and HMA CF formation in rats consuming sorghum bran may have resulted through the differential actions of the sorghum brans on endogenous antioxidant enzymes, which may affect colonocyte proliferation and apoptosis.

DEDICATION

In honor of the Lord Jesus Christ,
Who has sustained me throughout the early years,
Who will give me the hope to carry on in the later years.
Your unconditional grace and love overwhelm me.

To Him who sits on the throne and to the Lamb,
Be praise and honor and glory and power,
Forever and ever. Amen.

ACKNOWLEDGEMENTS

I would like to convey my earnest gratitude for my committee members. To my chair, mentor, and friend, Dr. Turner, thank you for all the time and knowledge that you have shared with me. Thank you for having confidence in me when I lacked it myself. Your encouragement and patience with me were invaluable. Thank you to Dr. Lupton for sharing with me your vast expertise and your kind words, a combination that makes you a wonderful educator. Thank you to Dr. Chapkin for demonstrating superior work ethic and for always challenging me to do my best. Finally, thank you to Dr. Rooney, my sorghum connoisseur, for all your research that paved the way for my study.

I would also like to express my utter appreciation for my lab family. Stella, you really are our lab mom as you go out of your way to offer time, advice, encouragement, snacks and love. I will always fondly remember the enriching conversations in your office and the sharing of delicious green sauce at Los Cucos. Kim, I cannot put into words how indispensable you have been to me these past two years. Whether it be in discussion of research or relationships, you were a constant reminder of Christ. I truly would not have made it without you. Lindsey, it has been great spending time with you this last year. Thanks for listening to me and sharing your life with me. Good luck with your future studies. You will do great. Youngmi and Hyemee, girls y'all are incredible. I have seen you grow so much these past two years in confidence and proficiency. You two truly are like sisters to me and I am sure that both of you will go on to do great things in life. Whether you end up in the States or in Korea, save a guest room for me.

To Ms. Lorenz and Dr. Talley, it was a pleasure working with the two of you. Both of you have been so encouraging to me. Thank you for your caring words and advice. And to many other professors and students at Texas A&M, thank you for the education and for taking the time to have a conversation or two with me.

Finally, I would like to communicate my love and gratefulness for my friends and family. Mom and Dad, you guys set a great example for us as children. Now, more than ever, I can appreciate all that you have taught me in life and love. I am blessed to have you as parents. Bob and Keyah, your generosity and love encourage me more than you know and I wish I told you that more often. Grandma, I love laughing with you. Your youthful spirit inspires me to live life unashamedly and with great joy. Meredith and Lindsay, you two are the best sisters a girl could ask for. Both of you have played an imperative role in the development of my character and I am thankful that you genuinely display your lives as an open book before me. I love you. Brandon and Chris, my brothers-in-law, you guys make me laugh so much, even when you are picking on me like a little sister. Both of you show profound integrity and dedication to your work and family. I could not have chosen better men for my sisters. To my friends, I wish I had space to address each of you individually. Thank you for always being there for me in times of emotional distress and sleepless nights, for the many miles driven to comfort me, for the encouraging words and gifts, and most of all for the laughter. Every single one of you are priceless to me. And last but not least, to Zachary, my encouragement, love, strength, and joy. You are my breath of fresh air at the end of these tumultuous two years. May God bless each of you for the impact you have had on my life.

TABLE OF CONTENTS

	Page
ABSTRACT	iii
DEDICATION	v
ACKNOWLEDGEMENTS	vi
TABLE OF CONTENTS	viii
LIST OF FIGURES.....	x
LIST OF TABLES	xii
 CHAPTER	
I INTRODUCTION.....	1
II LITERATURE REVIEW.....	4
Promotion of Colon Carcinogenesis	4
Aberrant Crypts	5
Proliferation and Apoptosis.....	5
Reactive Oxygen Species and Endogenous Antioxidants.....	7
Sorghum and Its Chemoprotective Capability	8
Hypothesis	11
Specific Aims	12
III MATERIALS AND METHODS	13
Experimental Design	13
Experimental Diets	14
Sample Collection	15
Aberrant Crypts	16
Proliferation.....	17
Apoptosis.....	18
Antioxidant Enzyme Activity.....	19
Reduced and Oxidized Glutathione.....	20
Statistical Analysis	23

CHAPTER	Page
IV RESULTS.....	24
Food Intake, Weight Gain, and Feed Efficiency	24
Antioxidant Enzyme Activity.....	25
Reduced and Oxidized Glutathione.....	27
Proliferation.....	29
Apoptosis.....	33
Aberrant Crypts	36
Regressions Using Diet Antioxidant Activity	38
V DISCUSSION	40
VI SUMMARY AND CONCLUSIONS.....	48
Summary	48
Conclusions	48
Future Research.....	50
LITERATURE CITED	51
APPENDIX A: EXPERIMENTAL PROTOCOLS	59
APPENDIX B: DATA TABLES	91
VITA	95

LIST OF FIGURES

	Page
Figure 1 Examples of Bioactive Compounds	11
Figure 2 Experimental Timeline.....	14
Figure 3 Experimental Diet Groups.....	14
Figure 4 Sample Collection	16
Figure 5 Sample Images of Proliferation Measurements.....	17
Figure 6 Sample Images of Apoptosis Measurements	18
Figure 7 Sample Image of HPLC Analysis of Glutathione	22
Figure 8 Total Superoxide Dismutase Activity	25
Figure 9 Mitochondrial Superoxide Dismutase Activity.....	26
Figure 10 Catalase Activity	26
Figure 11 Glutathione Peroxidase Activity	27
Figure 12 Reduced Glutathione Levels	28
Figure 13 Oxidized Glutathione Levels.....	28
Figure 14 Reduced/Oxidized Glutathione Ratio.....	29
Figure 15 Number of Intensely Stained Cells for Proliferation.....	30
Figure 16 Proliferative Index.....	31
Figure 17 Proliferative Index of Middle Tertile	31
Figure 18 Proliferative Index of Bottom Tertile.....	32
Figure 19 Proliferative Zone.....	32

	Page
Figure 20 Number of Apoptotic Cells	34
Figure 21 Apoptotic Index.....	34
Figure 22 Apoptotic Index of Top Tertile	35
Figure 23 Apoptotic Index of Middle Tertile	35
Figure 24 Total Number of Aberrant Crypts	36
Figure 25 Total Number of Aberrant Crypts Foci	37
Figure 26 High Multiplicity Aberrant Crypt Foci	37
Figure 27 Total Number of Aberrant Crypts vs. Antioxidant Activity	39
Figure 28 High Multiplicity Aberrant Crypt Foci vs. Antioxidant Activity.....	39
Figure 29 Structure of Anthocyanidins and 3-Deoxyanthocyanidins.....	42
Figure 30 Antioxidant Enzyme Schemes.....	44
Figure 31 Potential Mechanisms Involved in Black and Brown Sorghum Effects.....	49
Figure 32 Apoptotic Index vs. Antioxidant Activity	94

LIST OF TABLES

	Page
Table 1 Nutrient Analysis of Sorghum Brans	15
Table 2 Composition of Experimental Diets	15
Table 3 Food Intake Data	24
Table 4 Diet Compound Analyses.....	38
Table 5 Weight Gain Data.....	91
Table 6 Feed Efficiency Data.....	91
Table 7 Crypt Height.....	92
Table 8 Total Number of Light Stained Cells in Proliferation.....	92
Table 9 Total Number of Stained Cells in Proliferation	93
Table 10 Total Proliferative Index	93
Table 11 Apoptotic Index of Bottom Tertile.....	94

CHAPTER I

INTRODUCTION

In the past decade, cancer passed heart disease as the leading cause of death among Americans under the age of 85 (1). Among cancer-related deaths, colon cancer is second to lung cancer as the primary cause of death (2). It is notably influenced by environmental factors, such as diet (3, 4). Research has shown that whole grain consumption is favorable in the prevention of diseases, such as gastrointestinal cancers (5). Whole grains provide a sufficient amount of dietary fiber, which acts as a bulking agent and its fermentation in the colon produces a lower pH and short chain fatty acids, both of which seem to be protective (6, 7). Schatzkin et al (8) found an inverse relationship with the consumption of whole grains and the relative risk of colorectal cancer among a cohort of men and women. However, when colorectal cancer risk was further examined at a dietary fiber level, no association was found. This suggests that other whole grain components might be working with fiber to produce the prevention of colorectal cancer.

Whole grains contain other health-promoting constituents such as vitamins, minerals, and bioactive compounds. Bioactive compounds are non-nutritive substances derived from plants that possess cholesterol-lowering properties, antioxidant capacity, and have the potential to be chemoprotective (9, 10). Perhaps these compounds are aiding in protection against colorectal cancer, either directly or through a synergistic

This thesis follows the style and form of The Journal of Nutrition.

effect with dietary fiber. Nevertheless, more research is needed in order to determine the precise mechanisms whereby whole grains contribute to colon cancer prevention.

In order to address this issue, we chose to investigate the chemoprotective properties of sorghum grain. Sorghum is a grain commonly consumed in parts of Africa and Asia, but its main use in the United States is for animal feed. It is a robust cereal, able to outperform other grains in environmental stress (11, 12). Sorghum contains assorted classes and levels of bioactive compounds in its bran, varying by type, making it an ideal candidate to study differences in effects of these compounds. *In vitro* measurements of antioxidant activity (ORAC) show that sorghum possesses significantly higher levels than fruits, such as blueberries and strawberries (9).

In the 1971, Burkitt (13) observed that on a world list of incidence rates for colorectal cancer, a population in Uganda was at the bottom, along with three other African populations just above, while Western populations showed up to ten times greater incidence rates. These African populations are the same groups who have been consuming sorghum as a staple in their diet for generations. He postulated that the removal of dietary fiber from diets in developed countries was the causative agent of the higher incidences of colorectal cancer. However, it is a possibility that this lower incidence of colorectal cancer attributable to African civilizations was more than just a dietary fiber effect.

In its history, sorghum has been associated with lower incidences of esophageal cancer in diverse parts of the world that consume it frequently (14, 15). However, these observations seen in esophageal cancer have yet to be explored with regard to other

cancer types even though investigation is merited. In fact, relatively little research exists concerning sorghum relative to human health in general when compared with other bioactive compound-containing foods, such as fruits and vegetables. Thus, more exploration of this grain is needed in order to clear up our understanding of colon cancer prevention with regard to consumption of whole grains, dietary fiber, and bioactive compounds.

CHAPTER II

LITERATURE REVIEW

Promotion of Colon Carcinogenesis. Colon carcinogenesis is a complex, multistep process in which specific histopathological transitions occur over an extended amount of time, eventually leading to a fully malignant state. Human tumors have demonstrated that mutations derived from genetic predispositions, environmental factors, or the interactions between the two are what seem to drive this process (16, 17). When oncogenes are activated, they promote the malignant phenotype of cancer, while at the same time they can inhibit important tumor-suppressor genes (18). For example, inhibition of the tumor-suppressor gene adenomatous polyposis coli (APC), which regulates oncogenic β -catenin, can facilitate the mutation of a normal intestinal epithelial cell to a preneoplastic lesion of colon cancer (17).

Once an initial mutation has occurred, altered cells have a selected growth advantage, allowing the transformed cell type to replicate and further promote colon carcinogenesis (19). However, chemoprotective agents could be introduced in this promotion stage in order to reverse the detrimental processes through repair mechanisms, such as DNA repair or programmed cell death. Thus, tactics for prevention, such as diet, are vital at this stage of colon carcinogenesis in order to avert preneoplastic lesions from developing (20).

Aberrant Crypts. Although there is debate about the validity of aberrant crypt foci (ACF) as a colon cancer biomarker (21), these are considered to be preneoplastic lesions and are used as a biomarker for carcinogenesis induced by azoxymethane (AOM) in rat colons. They are also found in individuals who are at high risk for developing colon cancer (22-25). As compared to measuring actual tumor incidence for an endpoint, ACF measurements decrease the duration needed for the animal studies and thus cost while still providing a consistent, quantitative approach for colon cancer risk assessment. Colonic tissue is stained with methylene blue and examined for crypts which exhibit increased size, irregular luminal opening, and thicker epithelial lining (26). ACF are specific to colon carcinogenesis and the quantity and multiplicity of ACF numerically increase over time as an indicator of colon cancer development in animals (22, 27, 28). On top of this, ACF colonocytes have been shown to exhibit an increase in proliferation and an antagonism towards apoptosis (29, 30).

Proliferation and Apoptosis. Apoptosis is a form of programmed cell death by which cells are removed from the body. On the other hand, proliferation is the process of normal cell growth, but when upregulated as in malignant cell types, it leads to unrestricted cell division and tumor formation. In fact, common features of adenomatous polyps are unrestricted division of cells and the failure of these cells to differentiate properly (19). In view of this, the dynamic balance between cell death and cell survival plays a normal physiological role in regards of the shaping of organs and digits as well as the development the nervous and immune system (31). This balance is

also vital for protection against diseases and when this balance is perturbed, pathogenesis occurs (6, 31-33). For example, an increase in cell death is associated with AIDS, Parkinson's disease, Alzheimer's disease, and others. Conversely, a suppression or inhibition of apoptosis allows cells with genetic abnormalities, such as occurs in cancer, to survive (31).

A study done on human colonic epithelium showed a relationship between transformation of normal tissue to carcinomas and inhibition of apoptosis (34). Shpitz et al (30) demonstrated increased proliferative activity as a characteristic at each stage of neoplastic colonic lesions from human specimens, ranging from aberrant crypt foci to adenocarcinomas. However, proliferation can be misleading because cell replication alone does not necessarily indicate carcinogenesis, but it allows for the increased possibility of mutagenesis (30, 35). Chang et al (36) previously demonstrated that apoptosis was the overall best indicator of colonic tumor development when comparing measurements of cell proliferation, differentiation, and apoptosis.

Apoptosis is a distinct process where the cell shrinks, chromatin condenses, membrane surfaces bleb, and the DNA fragments after which the apoptotic body is usually phagocytosed by surrounding cells (31, 37). Studies have shown that apoptosis can be mediated by reactive oxygen species (ROS) (38), yet ROS are also thought to promote carcinogenesis through interference with signal cascade systems (NF κ B, AP-1, MAPKs) and by induction of DNA damage (37, 39-41). Mitogen-activated protein kinases (MAPKs) can be activated by growth factors and external stimuli via signaling cascades to influence cell proliferation. The pathway in which they are involved also

includes proto-oncogene products, Ras and Raf-1, and thus they are associated with carcinogenesis (39). When inadequately regulated, transcription factors nuclear factor-kappa B (NFκB) and activator protein-1 (AP-1) are associated with tumor promotion in that they activate cell proliferation in cells that otherwise would not survive (40).

Reactive Oxygen Species and Endogenous Antioxidants. ROS include the superoxide anion ($O_2^{\cdot -}$), hydrogen peroxide (H_2O_2), and the hydroxyl radical ($\cdot OH$). They are formed as byproducts in metabolic processes throughout the body, especially in the mitochondria at the site of the electron transport chain. These molecules can be damaging to the DNA of the cell and can compromise cell integrity (42, 43). As a first line of defense, the body has an endogenous antioxidant defense system of enzymes that are imperative for the inhibition of mutagens and protection against oxidative injury (44).

There are three isoforms of the superoxide dismutase (SOD): cytosolic (Cu/Zn-SOD), mitochondrial (Mn-SOD), and extracellular (EC-SOD). Cu/Zn SOD has two identical subunits, each containing a copper and a zinc atom associated together with a histamine residue. Mn-SOD is a homotetramer containing one manganese on each subunit. EC-SOD is a tetrameric glycoprotein, containing copper and zinc found in the interstitial spaces and extracellular fluid (45).

SOD will transform the $O_2^{\cdot -}$ into H_2O_2 . Superoxide anion is a highly reactive molecule that cannot cross cell membranes while H_2O_2 is able to traverse membranes and interact with metals (Fe^{2+} or Cu^+) via the Fenton reaction to form hydroxyl radicals

(37). However, both catalase (CAT) and glutathione peroxidase (GPx) are able to quench H_2O_2 to prevent damage. CAT is a homotetramer containing one ferriprotoporphyrin ring and it efficiently catalyzes the reaction to transform H_2O_2 into water and molecular oxygen (46). GPx is also a homotetramer containing a selenocysteine in each subunit, which is crucial for its peroxidase activity, which reduces hydroperoxides with the aid of glutathione (37, 45). Glutathione (GSH) is a thiol belonging to the secondary defense system against free radicals. It can also be readily oxidized to the disulfide (GSSG). The redox state of glutathione is also an indicator of the redox status of the cell and decreased GSH is a marker of oxidative stress and pathological conditions (47).

ROS are generally understood to be disease-promoting; however, more data have shown that they can have beneficial functions such as playing a role in apoptosis (38, 48). Nevertheless, individuals that produce excess ROS could be at higher risk for developing cancer and would benefit from exogenous antioxidants, which are able to influence the level and activity of both ROS and endogenous antioxidants (38). Cellular antioxidants do not completely remove ROS from the cells, but they contribute to the balance needed in order for normal cell function to be maintained (48).

Sorghum and Its Chemoprotective Capability. Recent research has shown that the consumption of whole grains is beneficial in prevention of disease, including gastrointestinal cancers (5). In the past, this effect of whole grain has been attributed to dietary fiber and scientists have observed a lower risk of colon cancer in populations of

Africa and China who consume diets high in fiber-rich whole grains (13). However, short-term clinical research has shown inconsistent results in regard to this hypothesis (30). Recently, the idea of the interaction of all the whole grain components working synergistically to cause the effect, as opposed to dietary fiber working alone, was proposed (49). Whole grains contain bioactive compounds, which give rise to anti-cancer capabilities, including antioxidant activity. In order to study how these compounds could be working to improve chemoprevention, we decided to examine a staple grain of the populations where the original effect was observed.

Being that it is a robust grain in environmental stress, sorghum has remained a principal food in developing parts of Africa and Asia (11, 12). It is the fifth leading cereal crop in the world, yet in the United States we rarely consume it. Sorghum is used in some gluten-free products for treatment of celiac patients (50); however, most of the product is used for animal feed. Even in the scientific realm, relatively little research has been done concerning this grain in regards to human health (51). Though sorghum goes unrecognized for the most part, it offers great potential in the area of antioxidant capability and chemoprevention.

Sorghum contains various bioactive compounds such as phenolic compounds, plant sterols and policostanols (9, 52). Plant sterols can reduce cholesterol absorption and policostanols may inhibit endogenous cholesterol synthesis (51). Phenolic compounds, defined as a compound containing a benzene ring with one or more hydroxyl groups, fall into two major categories: phenolic acids (cinnamic and benzoic acid derivatives) and flavonoids (include tannins and anthocyanins). These compounds

can be concentrated by decorticating the sorghum grain, producing bran to be used in diet (9, 53).

Phenols present in cocoa, similar in structure to those in sorghum, have shown positive health benefits such as reducing blood pressure (54), atherosclerosis (55), and growth of human breast cancer cells (56). Various sorghum brans have demonstrated much higher oxygen radical absorbance capacity (ORAC) levels on a dry matter basis than those in beneficial fruits such as blueberries and strawberries (9). Previous data from our lab demonstrated that flavonoids similar to those found in sorghum that were isolated from citrus, apigenin and naringenin, were able to decrease the formation of high multiplicity aberrant crypt foci (ACF), increase apoptotic index, and naringenin was able to decrease proliferation (28, 57).

Sorghums can be classified based on their appearance and level of phenolic compounds (**Fig. 1**). White sorghums contain small amounts of phenols, mostly as bound phenolic acids esterified to cell walls. Bound phenolic acids are important for antioxidant activity in cereals with low levels of flavonoids. Black sorghums contain high levels of 3-deoxyanthocyanins, the two most common being apigenidin and luteolinidin (58, 59). The 3-deoxyanthocyanins contain two aromatic rings that are able to stabilize a free radical. They also lack a hydroxyl group at the 3 position which is believed to increase their stability at high pH (60). Brown sorghums contain high levels of condensed tannins, which produce astringency in foods and beverages, such as dark chocolate and wine (53). Brown sorghums also demonstrate the highest antioxidant activities when compared to non-tannin sorghums (9). Tannins show the highest level of

antioxidant activity *in vitro* when compared with all other natural antioxidants. This is because they possess a high number of aromatic rings with hydroxyl groups which can stabilize free radicals (9, 52).

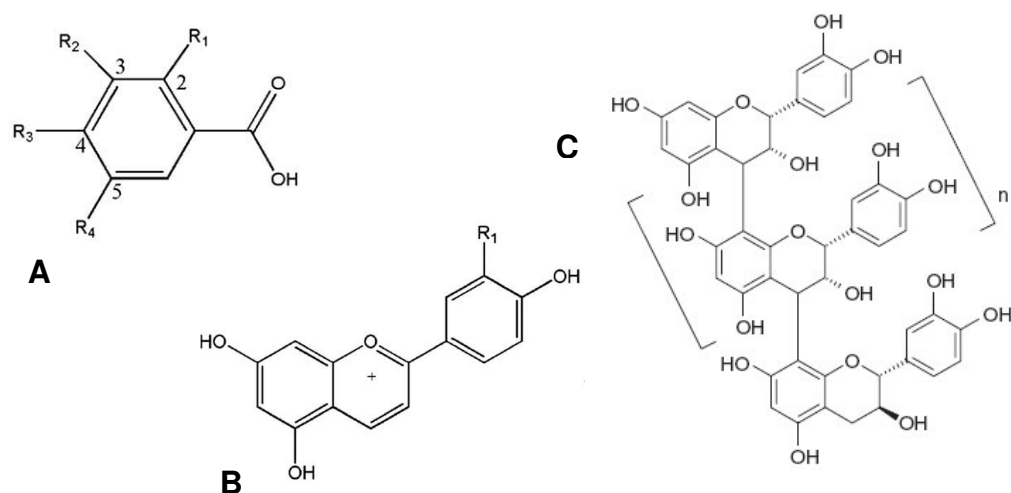


FIGURE 1 Examples of Bioactive Compounds. (A) Example of a phenolic acid, usually found in white sorghums. (B) Example of an anthocyanidin, typically found in black sorghums. (C) Example of a condensed tannin, found in brown sorghums. Pictures provided by Dr. L.W. Rooney.

Hypothesis. We hypothesized that the bioactive compounds present in the bran of brown (contains condensed tannins) and black (contains anthocyanins) sorghums would reduce the formation of preneoplastic lesions of colon cancer via changes in cell death and cell survival and/or colonic redox environment.

Specific Aims. The specific aims of this project were to:

- Determine if the level and/or type of bioactive compounds present in the sorghum brans would have an effect on development of preneoplastic lesions of colon cancer.
- Determine if diet effects on preneoplastic lesion development could be due to changes in cellular proliferation and apoptosis.
- Determine if the level and/or type of bioactive compounds contributed by the different sorghum brans affected the redox environment of the colonocyte as a result of adjustments in the activity of antioxidant enzymes (superoxide dismutase, catalase, glutathione peroxidase) or the level of reduced and oxidized glutathione.

CHAPTER III

MATERIALS AND METHODS

Experimental Design. The University Animal Care Committee of Texas A&M University approved the supervision put forth by the animal protocols of this study, which followed the guidelines of the National Institute of Health. This experiment used 40 male weanling (21-d old) Sprague-Dawley rats (Harlan Sprague Dawley, Houston, TX). Rats resided in a temperature (18-26° C) and humidity controlled environment with a 12 h light/dark cycle in individual raised wire cages. After arrival, rats were randomized into four different diet groups (n=10/group) subsequent to stratification by weight. Experimental diets and water were provided ad libitum. Following the first 3 wk of diet administration, the rats received their first subcutaneous azoxymethane (AOM; 15 mg/kg body weight; Sigma, St. Louis, MO) injection, which is a colon-specific carcinogen. One week later, they received a second subcutaneous AOM injection. The diets were provided for a total of 10 wk, after which the rats were killed using CO₂ asphyxiation and cervical dislocation (**Fig. 2**). Food intake and weight gain were recorded for each animal prior to the first AOM injection, 3 wk after the second AOM injection, and prior to killing.

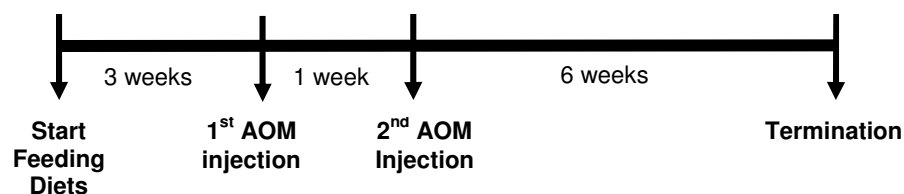


FIGURE 2 Experimental Timeline. Diets were provided for 3 wk, after which the first AOM injection was administered. After 1 wk, a second AOM injected was given. After 10 wk of the diets administration, the rats were terminated and samples were collected.

Experimental Diets. Semi-purified AIN-76A diets were provided containing 6% fiber from either cellulose, which was the control diet, or sorghum bran. Three types of sorghum bran were used: white, containing a trivial amount of bioactive compounds; black, containing an intermediate amount of bioactive compounds; and brown, containing the highest amount of bioactive compounds (**Fig. 3**). After the brans were analyzed for nutrient composition (**Table 1**), the diets were made equivalent in terms of macronutrient content (**Table 2**). All diets contained corn oil as the source of dietary lipid. The sorghum brans were prepared by decorticating the grain with a Prairie Regional Laboratory (PRL) Dehuller (52).

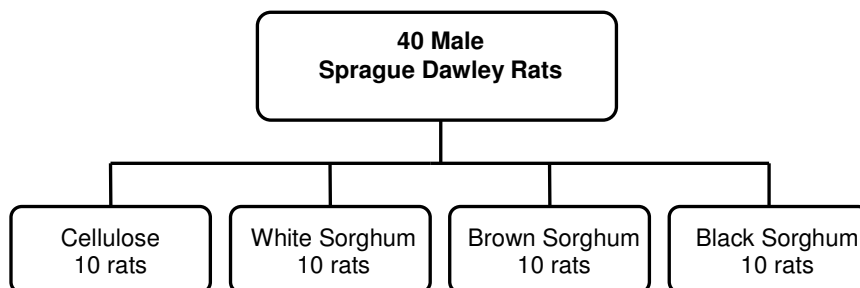


FIGURE 3 Experimental Diet Groups. Forty male Sprague-Dawley rats were split into four different diet groups with 10 rats in each group.

TABLE 1 Nutrient Analysis of Sorghum Brans

Ingredients	White Sorghum	Brown Sorghum	Black Sorghum
		%	
Protein	11.47	10.16	12.69
Lipid	7.01	6.89	2.48
Fiber	44.49	32.95	45.40
Carbohydrate	23.04	32.00	23.51
Ash	3.73	4.31	3.71
Moisture	10.26	13.69	12.21

TABLE 2 Composition of Experimental Diets

Ingredients	Control/ Cellulose	White Sorghum	Brown Sorghum	Black Sorghum
		<i>g/100 g</i>		
Diet Ingredients				
DL-methionine ¹	0.34	0.34	0.34	0.34
Mineral mix, AIN-76 A ¹	3.91	3.91	3.91	3.91
Vitamin mix, AIN-76 A ¹	1.12	1.12	1.12	1.12
Choline bitartrate ¹	0.22	0.22	0.22	0.22
Dextrose ¹	51.06	46.07	41.96	45.85
Casein ¹	22.35	20.80	20.50	20.67
Cellulose ¹	6.00	0.00	0.00	0.00
Sorghum bran ²	0.00	13.49	18.21	13.22
Corn Oil ¹	15.00	14.05	13.75	14.67
Macronutrient content				
Carbohydrate ³	51.06	49.19	47.79	48.96
Protein	22.35	22.35	22.35	22.35
Lipid	15.00	15.00	15.00	15.00
Fiber	6.00	6.00	6.00	6.00

¹Harlan Tekland, Madison, WI.

²Cereal Quality Lab, College Station, TX.

³Carbohydrate content varies because of the weight of ash and moisture in the sorghum bran fractions.

Sample Collection. After termination, the colon was removed and 2 cm were cut from the distal end of the colon (**Fig. 4**). One half was fixed in 4% paraformaldehyde and used for apoptosis while the other half was fixed in 70% ethanol and used for proliferation assays. The rest of the colon was cut longitudinally and rinsed with cold PBS. One half was flattened and fixed with 70% ethanol to be used for aberrant crypt foci (ACF) enumeration. The mucosal layer of the remaining half was scraped and a

small section (~5-10 μg) was snap frozen in liquid nitrogen and stored at -80°C for analysis of reduced/oxidized glutathione. The rest of the scraped mucosa was homogenized with protein buffer (described in appendix), centrifuged, and aliquots were stored at -80°C to use for antioxidant enzyme assays (superoxide dismutase, catalase, and glutathione peroxidase) (38).

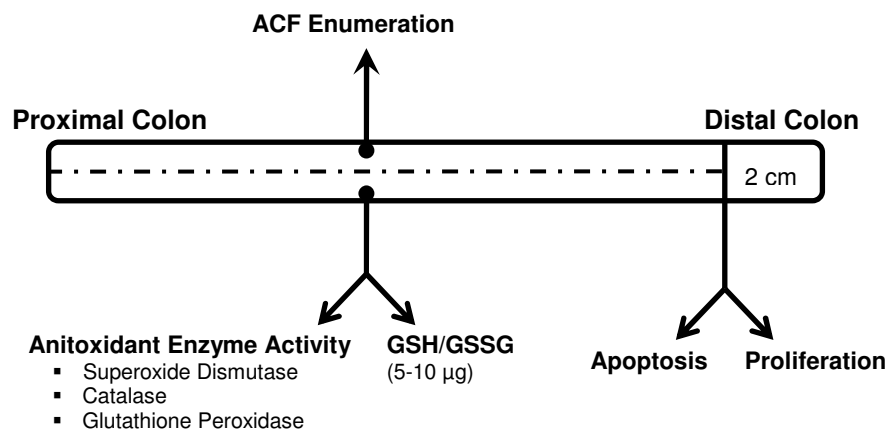


FIGURE 4 Sample Collection. Division of colon for data analysis.

Aberrant Crypts. One half of the distal colon was flattened and fixed with 70% ethanol for 24 h, stained with methylene blue (0.5%) and used for aberrant crypt foci (ACF) enumeration. After staining, the tissue was examined on a microscope at 40X and enumerated using the criteria of morphological characteristics previously described (28, 38). Tissue was examined for aberrant crypt foci, total number of aberrant crypts within the foci, and high multiplicity aberrant crypt foci, which contain four or more aberrant crypts.

Proliferation. Proliferation was assessed through detection of proliferating cell nuclear antigen (PCNA), which increases significantly during the S phase in mitosis because it is necessary for DNA replication and synthesis (61). We used a monoclonal PC-10 antibody (Signet Lab, Dedham, MA) and a Vectastain ABC Elite Kit (Vector Lab, Burlingame, CA). Negative controls were generated by using PBS in place of antibody during the assay. For every sample, the number of PCNA positive cells and their location was recorded in 25 crypt columns and the proliferative index was calculated as a percent of the number of labeled cells, both light and dark, per number of cells in the crypt column (**Fig. 5**). Proliferative zone was calculated as a percent of the highest labeled cell in the crypt per number of cells in the crypt column.

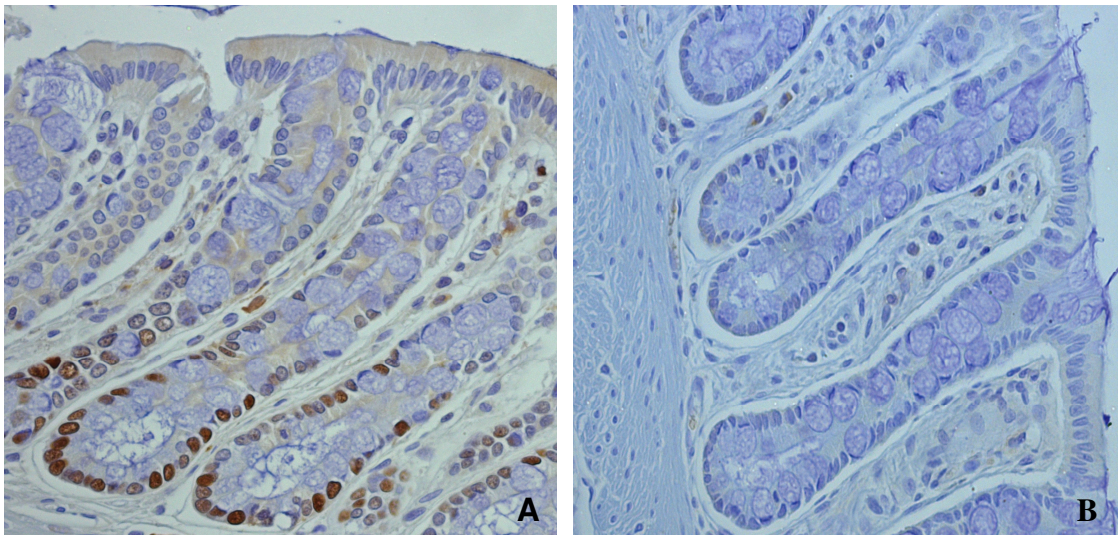


FIGURE 5 Sample Images of Proliferation Measurements. (A) Sample image of PCNA methodology for proliferation measurement. (B) Negative control generated by using PBS in place of antibody. Images at 40X.

Apoptosis. Tissues fixed in paraformaldehyde were used to determine apoptosis with the TUNEL assay (Intergen, Norcross, GA). Negative controls (not shown) were sections on each slide without TdT enzyme. Positive controls used colon sections from AOM-injected irradiated rats killed at 9 h after injection, known as a biological control for apoptosis in the bottom of the crypts (62). For every sample, apoptotic cells were identified by staining of diaminobenzidine tetrachloride (DAB) and appropriate morphological characteristics (**Fig. 6**). The crypt height was recorded from both sides of 25 crypt columns for each rat and the apoptotic index was calculated as the number of apoptotic cells/number of cells in the crypt column (62).

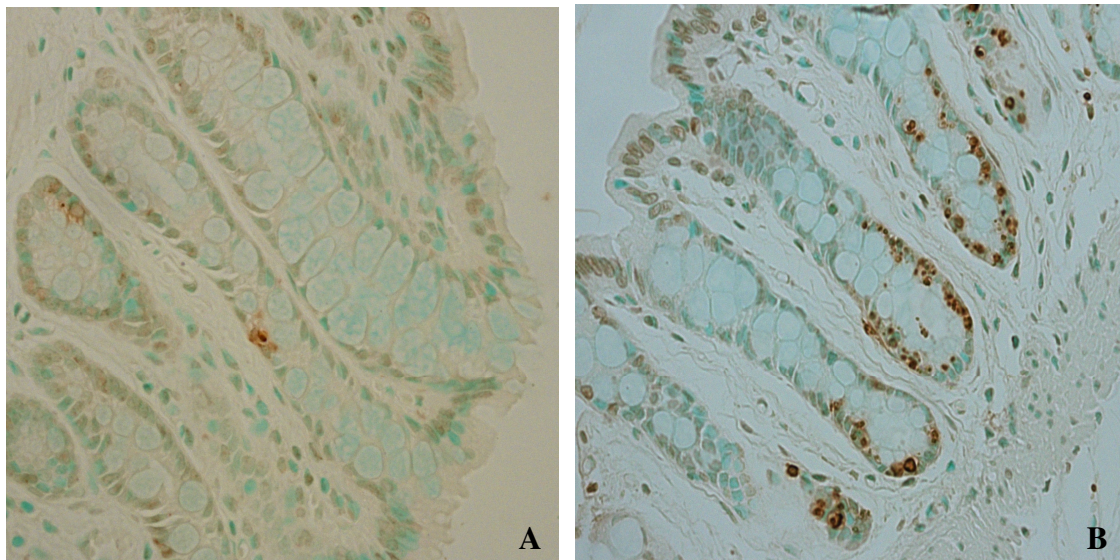


FIGURE 6 Sample Images of Apoptosis Measurements. (A) Sample image of TUNEL methodology for apoptosis measurement. (B) Positive control generated by using AOM-injected irradiated rats biologically known to have a high amount of apoptosis in the bottom of the crypt. Images at 40X.

Antioxidant Enzyme Activity. Cell lysates from the scraped mucosa of the colon were homogenized in protein buffer (described in appendix). Afterward, they were centrifuged for 30 min at 15,000 x g and aliquots were stored at -80°C to be used for antioxidant enzyme assays. Protein concentration was quantified using the Coomassie Plus Bradford assay kit (Pierce, Rockford, IL). Superoxide dismutase (SOD) activity, both total and mitochondrial, was measured by ELISA following the manufacturers' protocol (Cayman, Ann Arbor, MI). Ten microliters of cell lysate sample diluted in protein buffer (1:100) was combined with xanthine oxidase, producing superoxide radicals, which were detected by the tetrazolium salt used in the reaction. Potassium cyanide was added to another set of reactions to inhibit cytosolic (Cu/Zn) and extracellular (Fe) SOD, in order to detect the mitochondrial (Mn) SOD activity independently. Absorbance was read at 450 nm and a standard curve was used to determine SOD activity in the samples. Fifty percent dismutation of superoxide radical was defined as one unit of SOD activity (63). Catalase (CAT) and glutathione peroxidase (GPx) were measured by following the kit protocols (Calbiochem, San Diego, CA). In the CAT method, 20 µl of cell lysate sample diluted with protein buffer (1:40) was combined with methanol so that CAT could be measured based on its peroxidase activity with methanol in the presence of H₂O₂. Purpald was the chromogen used to spectrophotometrically measure the formaldehyde produced from the reaction at 540 nm. One unit of CAT activity was defined as the amount of enzyme needed to form 1.0 nmol of formaldehyde per min, which was obtained from the standard curve. Glutathione peroxidase (GPx) activity was an indirect measurement using 20 µl of cell

lysate sample diluted with sample buffer (1:20) coupled with the reaction of glutathione reductase, in which oxidized glutathione (GSSG) is converted back to reduced glutathione (GSH) using NADPH as the reducing equivalent. Oxidation of NADPH to NADP⁺ is associated with a decrease in absorbance at 340 nm. Conditions were such that GPx activity was rate limiting and therefore activity was directly proportional to decrease of A₃₄₀ as a function of time. All samples were run in triplicate along with standards provided on 96-well plates and read on a Spectra Max 250 microtiter plate reader (Molecular Devices, Sunnyvale, CA). The enzyme activities were normalized to the amount of protein using the Coomassie Plus Bradford assay and expressed as units of activity/mg protein (38).

Reduced and Oxidized Glutathione. Colonocyte reduced and oxidized glutathione concentrations were assessed using an HPLC method of Jones et al (1998) with modifications. Snap frozen tissue (~10 µg) was homogenized in 0.1 ml Solution A (1.05% L-serine, 0.1 mM sodium heparin, 2 mM bathophenanthroline disulfonate sodium salt, 11 mM iodoacetic acid, 80 mM boric acid, and 20 mM sodium tetraborate) plus 0.1 ml Solution B (1.2 mM perchloric acid and 200 mM boric acid). After homogenization, an additional 0.1 ml Solution A and 0.1 ml Solution B were added to the homogenates. The combined homogenates were centrifuged at 10,000 g for 1 min. The sample supernatant (150 µl) or 150 µl of GSH and GSSG standards (0, 50, 200, and 500 µM each) were combined with 30 µl of 40 mM iodoacetic acid and 100 µl of 1 M KOH/1.6 M potassium tetraborate (pH ~9.0). Subsequently, 150 µl of 75 mM dansyl

chloride was added. Both the samples and standards were vortexed and kept in dark at room temperature for 16 h, after which 250 μ l chloroform was added. The final mixture was centrifuged at 10,000 g for 1 min and 100 μ l of the supernatant fluid (dansyl derivatives) was transferred to a micro-insert tube in a brown vial, with 25 μ l injected into a 3-aminopropyl column (5 μ m; 4.6 x 250 mm; Custom LC, Houston, TX). Reduced and oxidized glutathione were eluted from the column using Solvent A (0.8 M sodium acetate, 27% glacial acetic acid, and 63% methanol; pH 4.6) and Solvent B (80% Methanol) at the combined flow rate of 1.0 ml/min and the following gradient (0-10 min, 20% Solvent A; 30-33 min, 80% Solvent A; 33.1-38 min, 20% Solvent A). Fluorescence detection (Waters 2475 Multi λ Fluorescence Detector) was set at 590 nm excitation and 610 nm emission (0.0 to 7.5 min) to eliminate the appearance of amino acid peaks and at 335 nm excitation and 610 nm emission (7.5 to 38 min) for reduced and oxidized glutathione detection. Gain of the detection was set at 100 (0 to 32.2 min) for reduced glutathione detection and at 1000 (32.2 to 38 min) for oxidized glutathione detection. Reduced and oxidized glutathione were quantified based on peaks generated by standards (Sigma Chemicals, St. Louis, MO) using the MillenniumTM-32 Software and workstation (**Fig. 7**). Concentrations were expressed relative to the amount of protein in the sample as measured by the Coomassie Plus Bradford assay (Pierce, Rockford, IL).

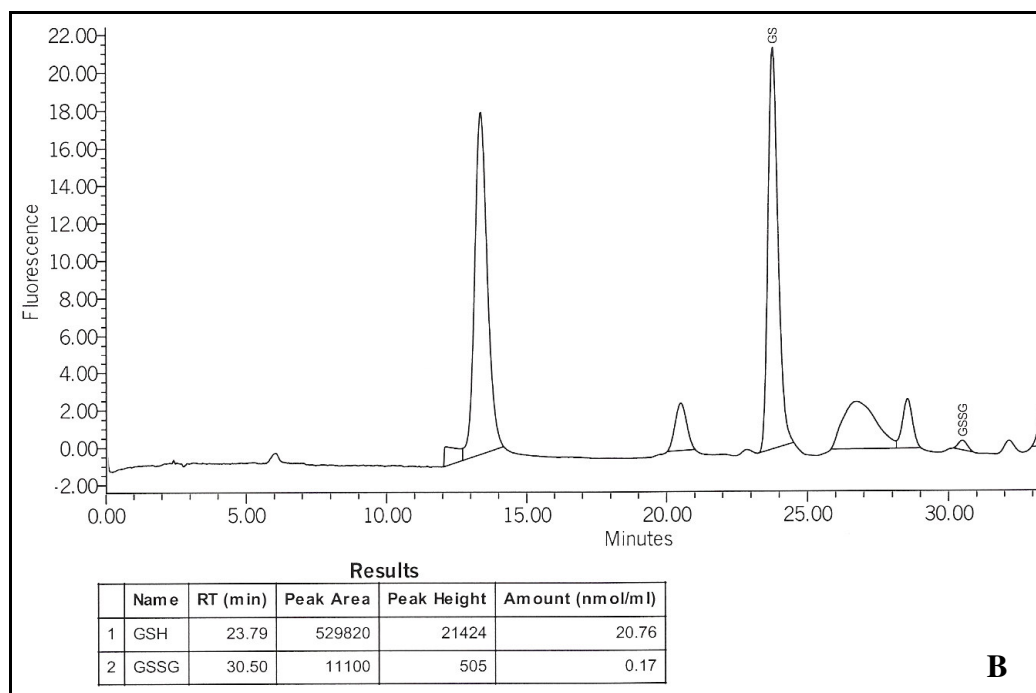
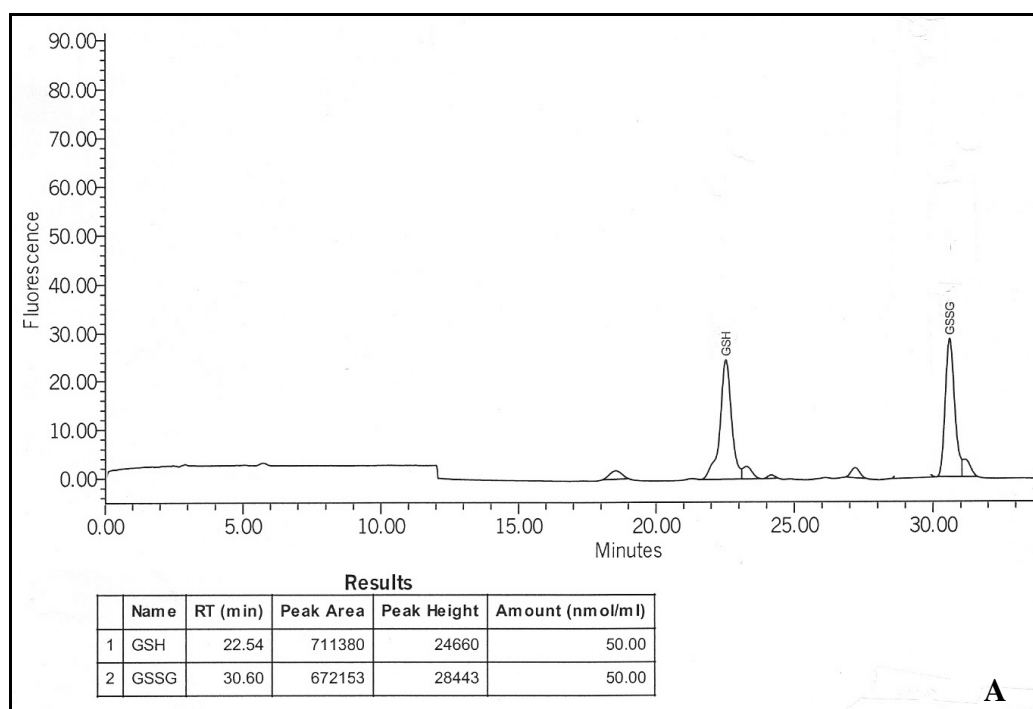


FIGURE 7 Sample Images of HPLC Analysis of Glutathione. Example of HPLC standard (A) and sample (B) trace for glutathione (GSH and GSSG) measurements.

Statistical Analysis. Data were analyzed using one-way analysis of variance (ANOVA) in SAS 9.1 (SAS Institute, Inc.) considering a p-value of <0.05 as significant. Outliers were removed if necessary and transformations were performed if normality was skewed. A Wilcoxon-Rank Sums non-parametric test was used in SAS 9.1 to determine difference of tannin levels among diets. Log regressions were run in SAS 9.1 to identify the relationship of aberrant crypts, high multiplicity aberrant crypt foci, and apoptotic index with the antioxidant activity in the diet. Finally, to account for slight differences that might have occurred in food intake, weight gain, and feed efficiency, we used these as covariates in the analysis of our end phenotype, ACF to see if they might have influenced the data. These covariates did not alter the outcomes of those statistical analyses.

CHAPTER IV

RESULTS

Food Intake, Weight Gain, and Feed Efficiency. In order to account for the potential of sorghum brans to affect food intake and body weight gain, we measured both variables over a 48 hr time period at wk 2, 7, and 10. We also calculated feed efficiency, defined as body weight gain divided by food intake. The food intake of black sorghum rats was depressed at wk 7 (relative to white sorghum rats) and wk 10 (relative to both white and brown sorghum rats), while cellulose rats were intermediate (**Table 3**, $p < 0.02$). This slightly affected body weight gain and feed efficiency at wk 7, but apparent differences in those variables were resolved by wk 10 (see **Table 5** and **6** in appendix). Additionally, to account for slight differences that might have occurred in food intake, weight gain, and feed efficiency, we used these as covariates in the analyses of our end phenotype, ACF to see if they might have influenced the data. These covariates did not alter the outcomes of those statistical analyses.

TABLE 3 Food Intake Data¹

Diet	Food Intake		
	Wk 2	Wk 7	Wk 10
	<i>g/24 h</i>		
Cellulose	16.40 ± 0.410 ^a	18.16 ± 0.518 ^{a,b}	17.58 ± 0.410 ^{a,b}
White Sorghum	16.73 ± 0.410 ^a	19.00 ± 0.518 ^a	17.93 ± 0.410 ^a
Black Sorghum	16.14 ± 0.410 ^a	17.01 ± 0.518 ^b	16.59 ± 0.410 ^b
Brown Sorghum	16.91 ± 0.410 ^a	17.65 ± 0.518 ^{a,b}	17.84 ± 0.410 ^a

¹Average 24-hr food intake data of rats over 48 hr time period at wk 2, 7, and 10. Data are means ± SEM for n=10 rats/diet. Means without common letter differ ($p < 0.02$).

Antioxidant Enzyme Activity. The endogenous antioxidant defense system, composed of SOD, CAT, and GPx, is vital for regulation of the oxidative status of cells. We wanted to determine if the diet antioxidants affected the activity of these enzymes in the colon. The black sorghum diet group had greater total SOD activity when compared to all other groups (**Fig. 8**, $p < 0.04$). A similar trend was observed in mitochondrial SOD activity, yet there were no significant differences among the diet groups (**Fig. 9**). The white sorghum rats had increased CAT activity when compared to the cellulose rats (**Fig. 10**, $p < 0.02$), while the black and brown sorghum rat samples were intermediate. All sorghum rats, white ($p < 0.03$), black ($p < 0.04$) and brown ($p < 0.001$), had suppressed GPx activity relative to cellulose rats (**Fig. 11**).

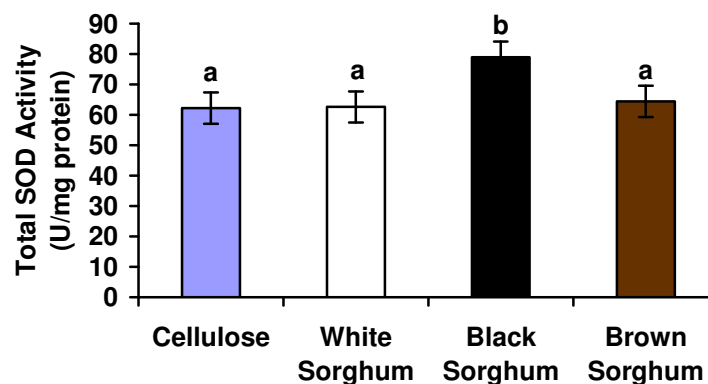


FIGURE 8 Total Superoxide Dismutase Activity. Rats provided a black sorghum diet had a greater level of total SOD activity when compared to rats in all other diet groups ($p < 0.04$). Data are means \pm SEM for $n=10$ rats/diet.

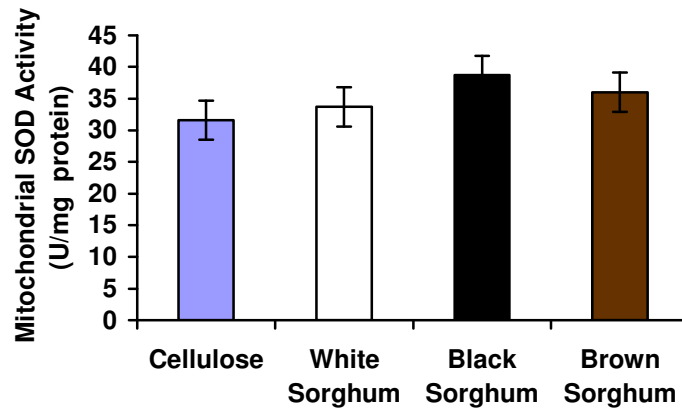


FIGURE 9 Mitochondrial Superoxide Dismutase Activity. No differences in mitochondrial SOD activity were seen among diet groups, yet the data showed a similar trend as seen in total SOD activity. Data are means \pm SEM for n=10 rats/diet.

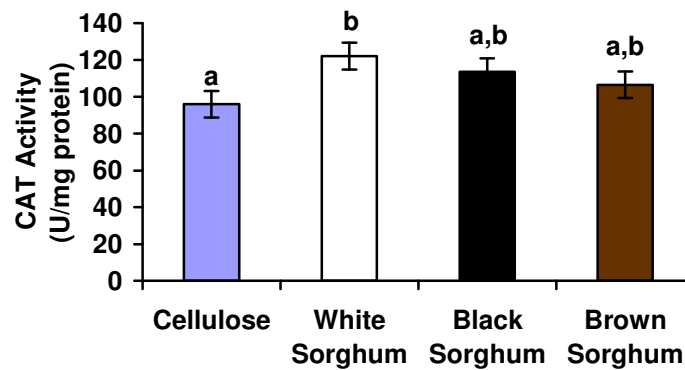


FIGURE 10 Catalase Activity. Rats provided a white sorghum diet had a greater level of CAT activity when compared to rats provided a cellulose diet ($p < 0.02$). Black and brown sorghum groups were intermediate. Data are means \pm SEM for n=10 rats/diet.

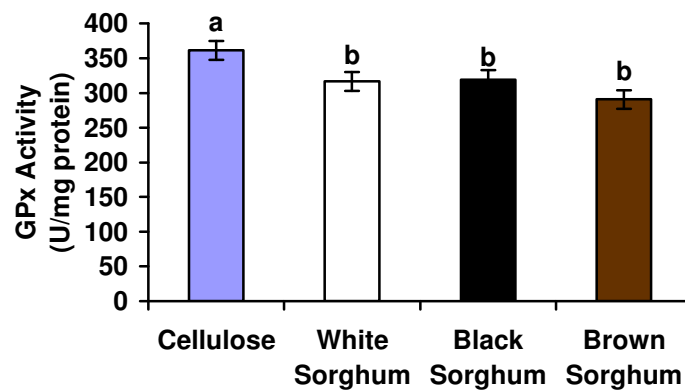


FIGURE 11 Glutathione Peroxidase Activity. All sorghum rats, white ($p < 0.03$), black ($p < 0.04$), and brown ($p < 0.001$) had a suppressed level of GPx activity when compared to rats provided a cellulose diet. Data are means \pm SEM for $n=10$ rats/diet.

Reduced and Oxidized Glutathione. The ratio of reduced (GSH) and oxidized (GSSG) glutathione is a good indicator of redox status (47). The level of reduced glutathione (**Fig. 12**), oxidized glutathione (**Fig. 13**), and the ratio of the two (**Fig. 14**) were measured. Although there were numerically greater concentrations of GSH and GSSG in the mucosa of all sorghum bran rats, there were no significant differences seen among the diet groups.

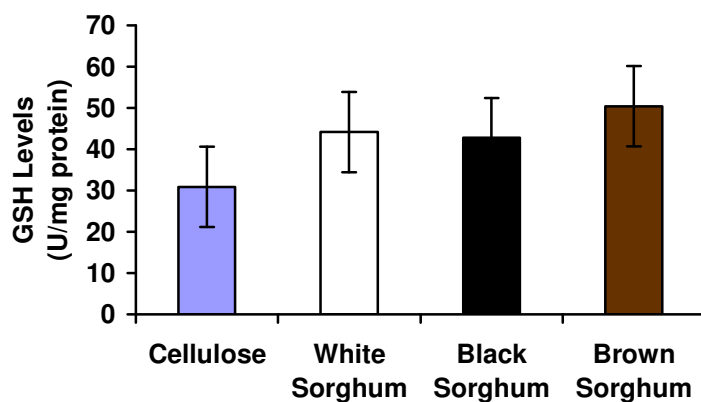


FIGURE 12 Reduced Glutathione Levels. AOM-injected rats were measured for level of reduced glutathione (GSH). No significant differences were observed. Data are means \pm SEM for n=10 rats/diet.

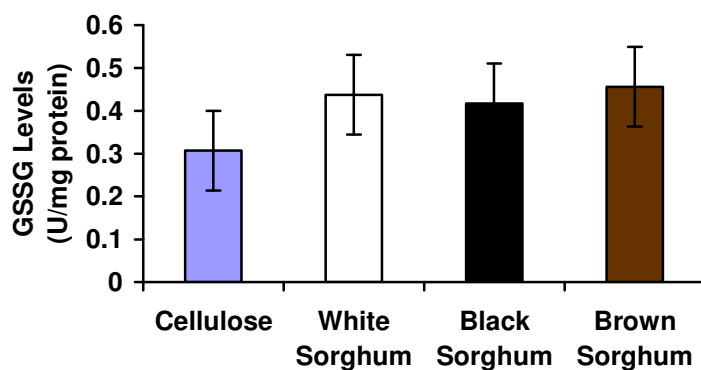


FIGURE 13 Oxidized Glutathione Levels. AOM-injected rats were measured for level of oxidized glutathione (GSSG). No significant differences were observed. Data are means \pm SEM for n=10 rats/diet.

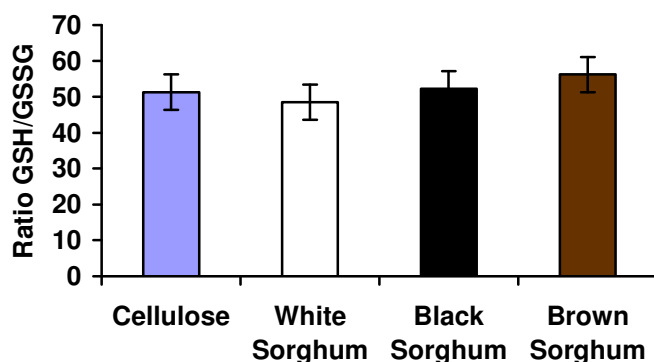


FIGURE 14 Reduced/Oxidized Glutathione Ratio. Ratio of GSH/GSSG was measured in AOM-injected rats. No significant differences were observed. Data are means \pm SEM for n=10 rats/diet.

Proliferation. Rapid cell division can become harmful if unregulated in colon carcinogenesis, leading to tumor formation. The distal colon (1 cm) was fixed in 70% ethanol and was embedded in paraffin in order to measure proliferation using PCNA as an indicator. Crypt height measurements were combined for proliferation and apoptosis and no meaningful differences were found among groups. The proliferative index was measured by the number intensely stained cells. Total number of intensely stained cells was higher in cellulose rats when compared to those in the black (**Fig. 15**, $p < 0.01$) sorghum groups.

Proliferative index, calculated by number of intensely stained cells divided by crypt height, was higher in cellulose rats when compared to those in the black (**Fig. 16**, $p < 0.01$) sorghum groups. Crypts were also separated into thirds in order to compare differences among each tertile. Proliferative index of the middle tertile was higher in cellulose rats when compared to those in the black (**Fig. 17**, $p < 0.009$) sorghum rats.

Proliferative index in bottom tertile was higher in cellulose rats when compared to those in the black (**Fig. 18**, $p < 0.014$) sorghum rats. The highest labeled cell in the crypt column is considered in order to determine proliferative zone. Proliferative zone was higher in cellulose rats when compared to those in the black (**Fig. 19**, $p < 0.04$) sorghum rats. There was no difference among diet groups in consideration of lightly stained cells.

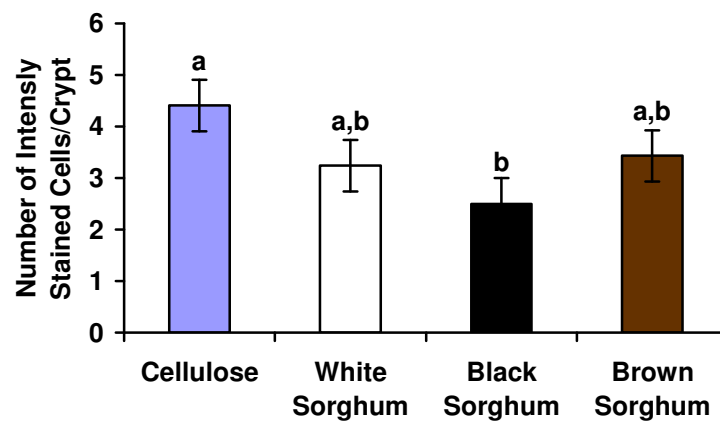


FIGURE 15 Number of Intensely Stained Cells for Proliferation. Absolute number of intensely stained cells per crypt was higher in cellulose rats when compared to those in the black ($p < 0.01$) sorghum rats. White and brown sorghum rats were intermediate. Data are means \pm SEM for $n=10$ rats/diet.

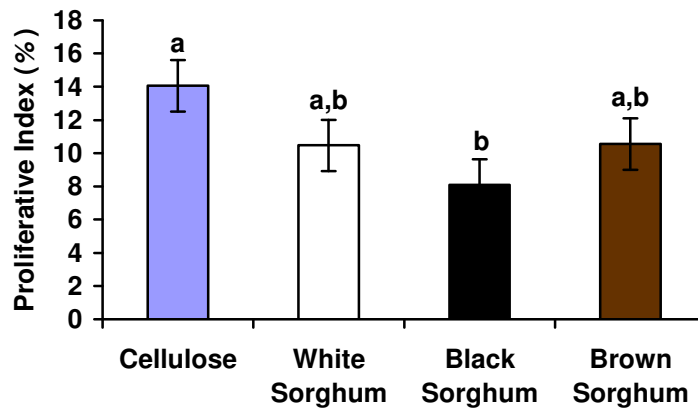


FIGURE 16 Proliferative Index. Proliferative index was measured as number of intensely labeled cells/crypt height (%). Proliferative index was higher in cellulose rats when compared to those in the black ($p < 0.01$) sorghum rats. White and brown sorghum rats were intermediate. Data are means \pm SEM for $n=10$ rats/diet.

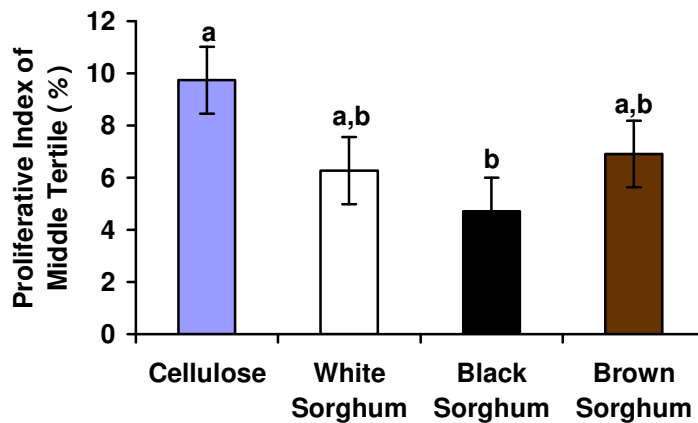


FIGURE 17 Proliferative Index of Middle Tertile. Proliferative index was measured as number of intensely labeled cells/total cells in tertile (%). Proliferative index of the middle tertile was higher in cellulose rats when compared to those in the black ($p < 0.009$) sorghum rats. White and brown sorghum rats were intermediate. Data are means \pm SEM for $n=10$ rats/diet.

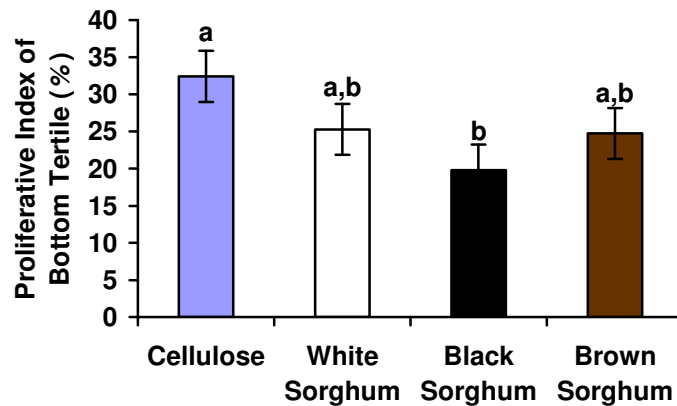


FIGURE 18 Proliferative Index of Bottom Tertile. Proliferative index was measured as number of intensely labeled cells/total cells in tertile (%). Proliferative index in bottom tertile was higher in cellulose rats when compared to those in the black ($p < 0.014$) sorghum rats. White and brown sorghum rats were intermediate. Data are means \pm SEM for $n=10$ rats/diet.

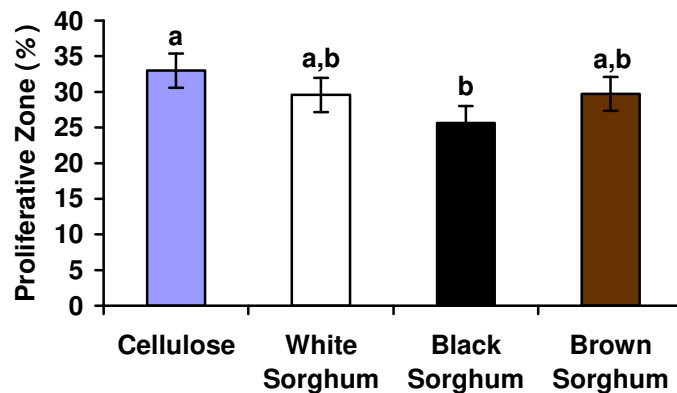


FIGURE 19 Proliferative Zone. Proliferative zone was measured as highest labeled cell/crypt height (%). Proliferative zone was higher in cellulose rats when compared to those in the black ($p < 0.04$) sorghum rats. White and brown sorghum rats were intermediate. Data are means \pm SEM for $n=10$ rats/diet.

Apoptosis. Programmed cell death, apoptosis, is a means of eradicating damaged cells, which otherwise could form tumors. The distal colon (1 cm) was fixed in 4% paraformaldehyde and was embedded in paraffin in order to measure apoptosis using the TUNEL assay. The total number of apoptotic cells was identified based on staining and morphological changes. Apoptotic index was calculated as total number of apoptotic cells per total cells in crypt height. The crypt was split into tertiles and the apoptotic index was recorded for each.

There were no differences in crypt height among different diet groups. The total number of apoptotic cells (**Fig. 20**, $p < 0.027$) as well as overall apoptotic index (**Fig. 21**, $p < 0.03$) was higher in brown sorghum rats when compared to cellulose rats. The apoptotic index in the top tertile was elevated in both black ($p < 0.0066$) and brown ($p < 0.034$) sorghum rats (**Fig. 22**). The apoptotic index in the middle tertile was higher in brown sorghum rats when compared to cellulose rats (**Fig. 23**, $p < 0.029$). Apoptotic index in the bottom tertile was not significant due to the low number of apoptotic cells in the bottom of the crypt.

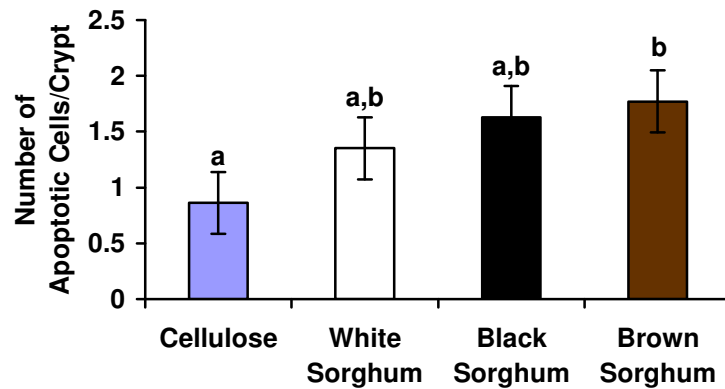


FIGURE 20 Number of Apoptotic Cells. The absolute number of apoptotic cells was recorded in colonic crypts. Brown sorghum rats had a higher number ($p < 0.027$) of apoptotic cells per crypt than did cellulose rats. Data are means \pm SEM for $n=10$ rats/diet.

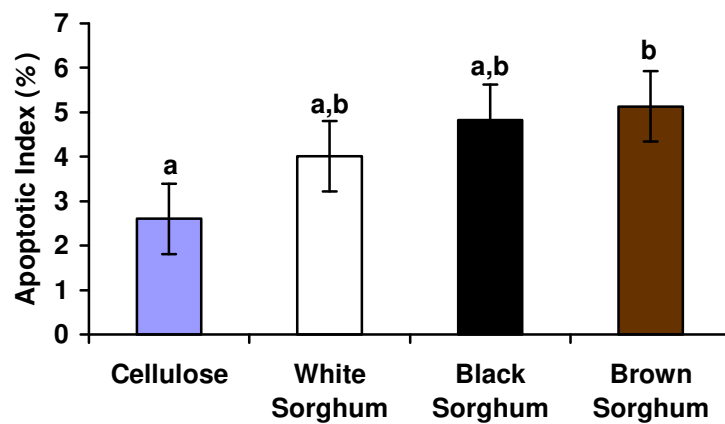


FIGURE 21 Apoptotic Index. The apoptotic index was calculated as total number of apoptotic cells in a crypt column/crypt column cell number. Brown sorghum rats had a higher apoptotic index ($p < 0.03$) than did cellulose rats. Data are means \pm SEM for $n=10$ rats/diet.

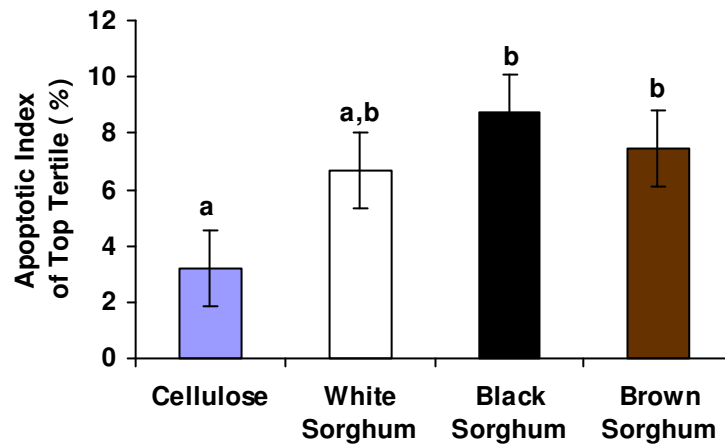


FIGURE 22 Apoptotic Index of Top Tertile. The apoptotic index was calculated as total number of apoptotic cells in a crypt column/crypt column cell number in each tertile of the crypt. Both black ($p < 0.0066$) and brown ($p < 0.034$) sorghum rats had a higher apoptotic index than did cellulose rats. Data are means \pm SEM for $n=10$ rats/diet.

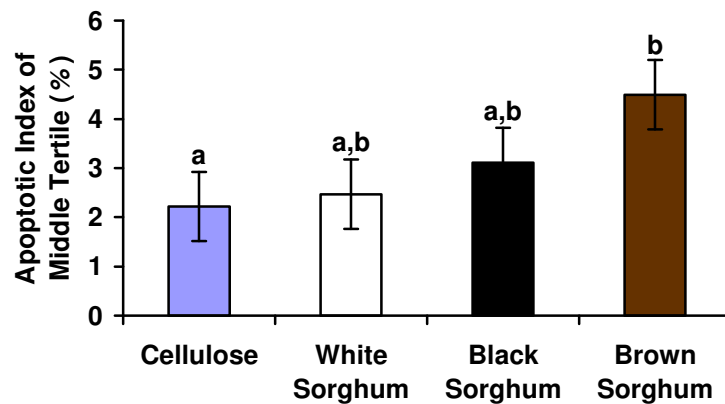


FIGURE 23 Apoptotic Index of Middle Tertile. The apoptotic index was calculated as total number of apoptotic cells in a crypt column/crypt column cell number in each tertile of the crypt. Brown sorghum rats had higher apoptotic index ($p < 0.029$) than did cellulose rats. Data are means \pm SEM for $n=10$ rats/diet.

Aberrant Crypts. Aberrant crypts were measured in order to establish the overall effect of the diet groups as a protective measure against colon carcinogenesis. The total number of aberrant crypts was significantly lower in rats consuming black ($p < 0.05$) and brown ($p < 0.0017$) sorghum diets when compared to those consuming the cellulose diet; the brown sorghum group ($p < 0.03$) was also lower when compared to white sorghum group (**Fig. 24**). The number of aberrant crypt foci was lower in rats consuming brown sorghum as compared to those consuming cellulose (**Fig. 25**, $p < 0.005$). High multiplicity aberrant crypt foci showed the same trend as was seen in total aberrant crypt data in which rats consuming black ($p < 0.03$) and brown ($p < 0.0002$) sorghum diets had fewer numbers when compared to those consuming the cellulose diet. Brown sorghum rats ($p < 0.001$) also showed fewer HMAF than white sorghum rats (**Fig. 26**).

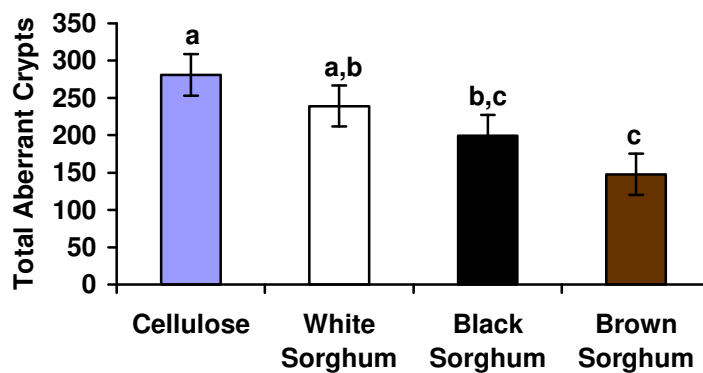


FIGURE 24 Total Number of Aberrant Crypts. AOM-injected rats were measured for total number of aberrant crypts (AC). Total AC were lower in animals from the brown ($p < 0.0017$) and black ($p < 0.05$) sorghum group as compared to those in the cellulose group. Animals in brown group had less total AC as compared to white sorghum animals ($p < 0.03$). Data are means \pm SEM for $n=10$ rats/diet.

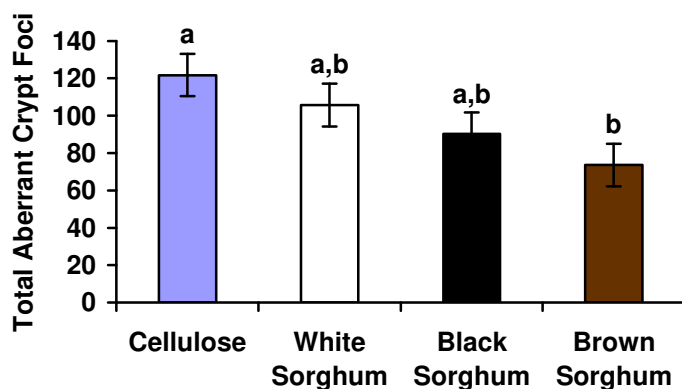


FIGURE 25 Total Number of Aberrant Crypt Foci. AOM-injected rats were measured for total number of aberrant crypt foci (ACF). Total ACF were lower in animals from the brown ($p < 0.005$) sorghum group as compared to those in the cellulose group. Data are means \pm SEM for $n=10$ rats/diet.

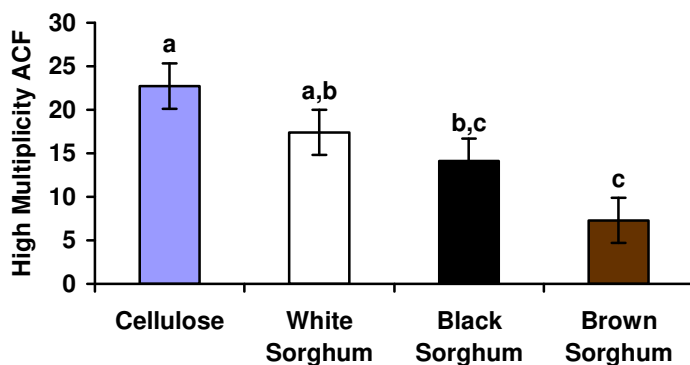


FIGURE 26 High Multiplicity Aberrant Crypt Foci. High multiplicity aberrant crypt foci (HMACF) were lower in AOM-injected rats from the brown ($p < 0.0002$) and black ($p < 0.03$) sorghum groups as compared to those in the cellulose group. Animals in the brown group had fewer HMACF compared to white sorghum animals ($p < 0.01$). Data are means \pm SEM for $n=10$ rats/diet.

Regressions Using Diet Antioxidant Activity. In order to compare the antioxidant potential of the experimental diets, we measured the content of phenols and tannins and the actual antioxidant activity (ABTS) of the diets themselves (**Table 4**). When we compared antioxidant activity of the diets with the total number of aberrant crypts (**Fig. 27**, $p < 0.02$) and high multiplicity aberrant crypt foci (**Fig. 28**, $p < 0.04$) in the animals, we observed an exponential decrease in aberrant crypts as a function of increasing antioxidant activity. We also compared the diet antioxidant activity with apoptotic index. While there was a tendency for apoptotic index to be higher in rats consuming diets with higher antioxidant activity, this relationship was not statistically significant (see **Fig. 32** in appendix, $p < 0.07$).

TABLE 4 Diet Compound Analyses^{1,4}

Diet	Phenol	Tannin ²	ABTS
	<i>mg GAE/g</i> ³	<i>mg CE/g</i> ³	<i>μmol TE</i> ³
Cellulose	0.281 ± 0.021 ^a	0.072 ± 0.042 ^a	7.893 ± 0.144 ^a
White Sorghum	0.776 ± 0.035 ^b	0.069 ± 0.041 ^a	14.88 ± 0.271 ^b
Black Sorghum	4.986 ± 0.092 ^c	ND	85.61 ± 1.558 ^c
Brown Sorghum	14.15 ± 0.148 ^d	19.03 ± 1.304 ^b	226.4 ± 4.121 ^d

¹Data are means ± SEM for n=10 /diet. Means in columns with superscripts without a common letter differ, $P < 0.001$ unless denoted otherwise. Measured by one-way ANOVA test.

²Mean in columns without a common letter differ, $P < 0.002$. Measured by a Wilcoxon rank-sums non-parametric test.

³GAE, gallic acid equivalents; CE, catechin equivalents; TE, trolox equivalents.

⁴Samples were analyzed by the Cereal Quality Lab at Texas A&M University.

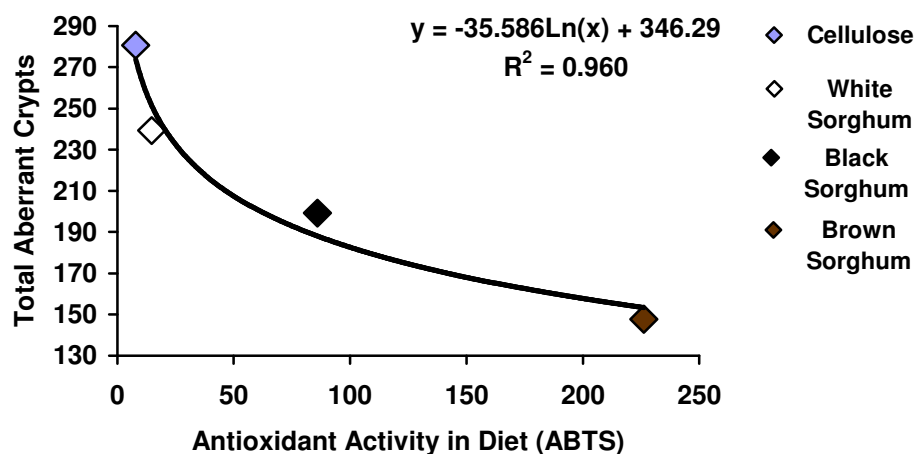


FIGURE 27 Total Number of Aberrant Crypts vs. Antioxidant Activity. Four experimental diets were fed to 40 AOM-injected rats (n=10/diet). The antioxidant activity of the diets was measured by 2,2'-azino-bis(3-ethylbenzthiazoline-6-sulphonic acid (ABTS) method. Aberrant crypts were counted from the distal colon of all animals. A trend was observed in which the total number of aberrant crypts decreased as the antioxidant activity of the diet increased ($p < 0.021$).

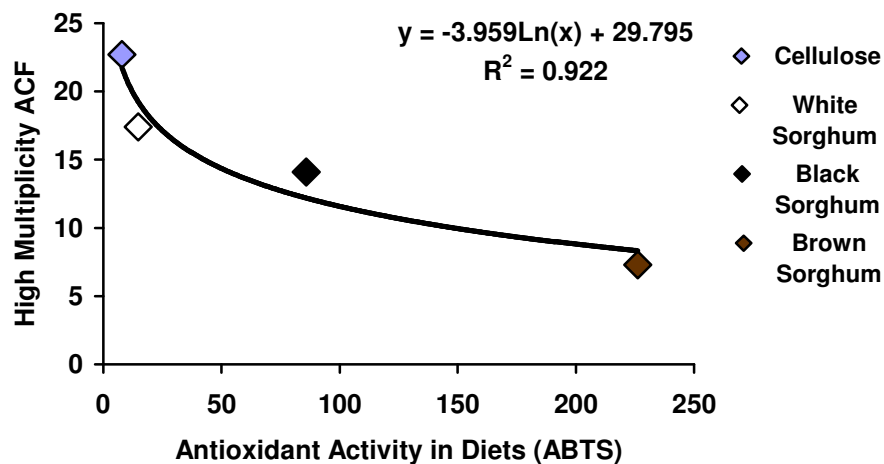


FIGURE 28 High Multiplicity Aberrant Crypt Foci vs. Antioxidant Activity. Four experimental diets were fed to 40 AOM-injected rats (n=10/diet). The antioxidant activity of the diets was measured by 2,2'-azino-bis(3-ethylbenzthiazoline-6-sulphonic acid (ABTS) method. HMACF were counted from the distal colon of all animals. A trend was observed in which the total number of HMACF decreased as the antioxidant activity of the diet increased ($p < 0.04$).

CHAPTER V

DISCUSSION

As stated, we chose to study sorghum in a colon cancer model due to previous observations seen in which certain populations had decreased incidence of esophageal cancers, and these same populations have been identified with lower risk of colon cancer (9, 13). It was postulated that a dietary fiber effect alone accounted for lowered colon cancer risk; however, other trials have shown inconsistent data based on that hypothesis (30). It is known that grains, in their entirety, contain other components besides dietary fiber and these also could be contributing to the previous observations. Sorghum in particular, varying by type, contains certain bioactive compounds (phenolic acids, anthocyanidins, and tannins) whose actions *in vivo* need to be characterized in order to clear up our understanding of whole grain chemoprotection in colon carcinogenesis.

In the past, tannins were shown to bind proteins and decrease protein digestibility and feed efficiency in animals (64, 65). However, we did not observe an effect on weight gain, food intake, or feed efficiency in the tannin (brown) sorghum rats. We saw a slight decrease in food intake in the black sorghum rats at the end of the study, though this did not affect weight gain or feed efficiency.

We did observe a sorghum effect with respect to the preneoplastic lesions of colon cancer, ACF. Both the black and brown sorghum rats had significantly fewer total aberrant crypts and high multiplicity aberrant crypt foci when compared to cellulose rats. Rooney et al (7) previously studied the effect of white and brown sorghum bran on

colonic physiology in male Sprague-Dawley rats. They found that both sorghums act as great bulking agents. In relation to control, both white and brown sorghum brans did not cause a decrease in colonic pH, which is attributed with enhanced carcinogenesis (66, 67). They postulated that brown sorghum bran could have a positive influence on the colon. This was confirmed by our study in which rats consuming brown sorghum bran had the lowest number of ACF.

The black and the brown sorghum brans contain high amounts of 3-deoxyanthocyanidins and tannins, respectively, and they are the two diets measured with the highest antioxidant activity by ABTS. We further analyzed this observation by running log regressions of diet antioxidant activity with total aberrant crypt and high multiplicity aberrant crypt data. Both regressions show a strong inverse relationship and suggest that the ability of these diets to suppress colon carcinogenesis could be linked to their high antioxidant potential and/or the other biological activities of the compounds that generate the antioxidant activity.

Significant alterations to cell cycle response were also observed in both the black and brown sorghum rats. In the case of proliferation, the black sorghum rats had fewer absolute numbers of proliferating cells and a lower proliferative zone, and proliferative index overall and in the middle and bottom tertiles. Shih et al (68) tested chemoprotective properties of 3-deoxyanthocyanidins, luteolinidin and apigenidin, the two main anthocyanidins in black sorghum. These compounds were able to reduce viability of human cancer cell lines (leukemia HL-60 and hepatoma HepG2) and were able to achieve this more effectively than their anthocyanidin counterparts (cyanidin and

pelargonidin). This suggests that inhibition of cancer cell viability by 3-deoxyanthocyanidins may be enhanced by dehydroxylation at the C-3 position on the compounds. Luteolinidin was more effective than apigenidin at inhibition of cancer cell growth.

Hou et al (69) found that certain anthocyanidins (delphinidin, petunidin, and cyanidin, **Fig. 29**) contributed to the inhibition of tumorigenesis via the blocking of MAPK pathway activation and AP-1 activation in JB6 mouse cells. It was hypothesized that these compounds were able to block AP-1 activation due to the ortho-dihydroxyphenyl structure on the B ring because the three compounds that caused inhibition are the only compounds that contain this particular structure.

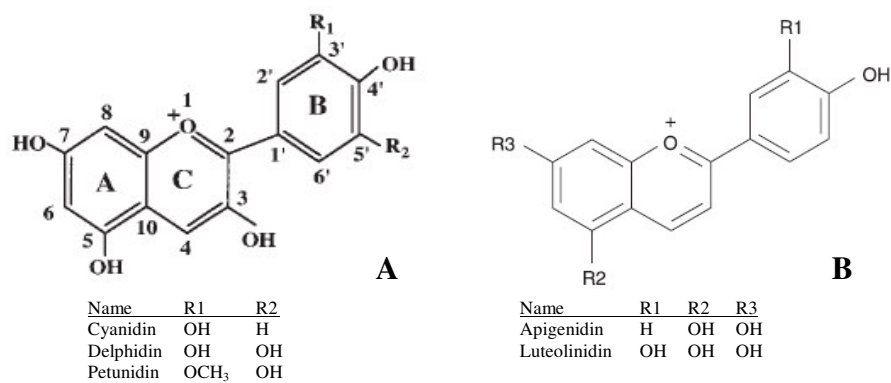


FIGURE 29 Structure of Anthocyanidins and 3-Deoxyanthocyanidins. (A) Structure of common anthocyanidins. The ortho-dihydroxyphenyl structure on the B ring is hypothesized to be involved in AP-1 inactivation via structure-activity relationships. (B) Structure of common 3-deoxyanthocyanidins in black sorghum. Luteolinidin contains the ortho-dihydroxyphenyl structure discussed in Hou's paper.

Furthermore, Hou et al (69) found that AP-1 activity was also blocked by SOD activity, but not by CAT. It appears that the superoxide anion is involved in the activation of AP-1 activity. Hou et al (69) found a synergistic affect of AP-1 inactivation when SOD activity and anthocyanidins were combined. Interestingly, we also saw an increased amount of SOD activity in the colons of rats eating the black sorghum diet, which occurred in conjunction with a decreased amount of proliferation in these animals. Black sorghums also contain a high amount of 3-deoxyanthocyanidin luteolinidin, which has the same structure as anthocyanidins above, but without a hydroxyl group on the third carbon of the C ring (**Fig. 29**). Luteolinidin maintains the ortho-dihydroxyphenyl structure. Perhaps this may contribute to its greater cytotoxicity against cancer cells over apigenidin and conceivably our anticarcinogenic observations are also due to the structure-activity relationship reported by Hou et al (69).

When compared to cellulose, brown sorghum rats demonstrated an elevated amount of apoptotic cells and a higher apoptotic index, contributing to their ability to suppress tumorigenesis. Black sorghum rats showed higher apoptotic index compared to cellulose rats in the top tertile, but not overall. Chang et al (36) saw among measurements of proliferation, differentiation, and apoptosis, that apoptosis was the best indicator of tumorogenesis. Though black sorghum rats showed a significant suppression of proliferation, the enhanced apoptotic index in brown sorghum rats was a better indicator of cancer prevention, confirmed by the fact that they had the lowest amount of aberrant crypts.

Previous studies have shown the ability of condensed tannins to induce apoptosis in human colon cancer cells (70, 71). Al-Ayyoubi et al (72) showed an induction of tumor-suppressor gene p53 in HCT-116 p53 +/+ colon cancer cells with treatment of gallotannin and an induction of apoptosis in HCT-116 p53 -/- cells. In addition, condensed tannins from grape seeds induced apoptosis through inhibition of anti-apoptotic PI3-K activity in CaCo2 cells (73). The condensed tannins found in our brown sorghum diet could be inducing apoptosis via similar pathways in order to prevent tumorigenesis.

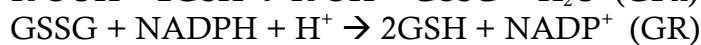
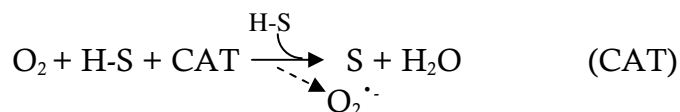
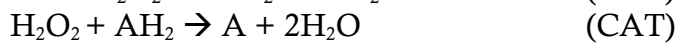
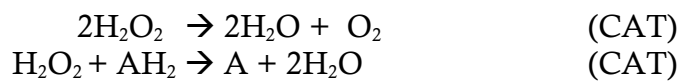
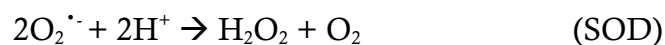


FIGURE 30 Antioxidant Enzyme Schemes. Reaction scheme of antioxidant enzymes and glutathione. SOD, superoxide dismutase; CAT, catalase; A, acid; H-S, reducing substrate; GPx, glutathione peroxidase; GR, glutathione reductase.

In order to see how a high load of exogenous antioxidants might affect the endogenous antioxidant environment (**Fig. 30**), we measured three antioxidant enzymes and a redox indicator, glutathione. SOD activity was elevated in black sorghum rats when compared to cellulose rats. CAT activity was elevated in white sorghum rats when

compared to cellulose rats. GPx activity was suppressed in all sorghum rats when compared to cellulose rats. However, no significant changes were seen in actual redox environment as indicated by measurements of reduced and oxidized glutathione.

As discussed earlier, SOD has been shown to help inhibit AP-1 activity in a synergistic manner with certain anthocyanidins (69). Given that luteolinidin, a main 3-deoxyanthocyanidin in black sorghum, has a comparable structure to these anthocyanidins, this gives rise to a potential mechanism of action for the black sorghum diet. The 3-deoxyanthocyanidin could work in conjunction with SOD to inhibit AP-1 activity, proliferation, and carcinogenesis.

Recently, CAT has been attributed with a third, previously unrecognized oxidase activity (74). In low concentrations of H_2O_2 , oxygen-dependent CAT oxidase activity will catalyze the oxidation of reducing substrates (75). However, an incomplete reaction could result in the formation of radical intermediates and superoxide anion (see **Fig. 30**). Vetranon et al (74) showed that phenolic acids, ferulic and vanillic acids, were competitive inhibitors for substrate 10-acetyl-3,7 dihydroxyphenoxazine used in their characterization of the catalase oxidase activity. Due to the speculation that catalase oxidase could be important in activating carcinogens, such as benzidine, to form further carcinogenic derivatives, they postulated that this competitive inhibition by phenols could aid in anti-cancer activity.

Perhaps the measured peroxidative activity of CAT in our study was enhanced in the white sorghum (contains phenolic acids) rats because the phenolic acids were competitive inhibitors of the oxidase function of the enzyme. The phenolic acids

increased the K_m of the oxidase activity, making it less effective and H_2O_2 a more competitive substrate to enhance the other functions of CAT, which we measured.

Higher levels of GPx activity were found in colonic tumor tissue when compared with normal tissue because the tumor was exposed to more oxidative stress and there was a need to enhance an antioxidant defense against this (44). The suppression of GPx in all sorghum rats when compared to cellulose suggests an ability of the cells to handle a higher amount of oxidative injury that occurred with tumor initiation. Perhaps this was due to the high amount of exogenous antioxidants present in the colon that were provided by the diets. To a certain extent, this protection against potential oxidative injury enabled the tissue to form fewer aberrant crypts in the sorghum rats.

In all of this, no significant overall change in redox status was seen in the tissue as measured by reduced and oxidized glutathione at the end of the study. This suggests that while there are shifts in antioxidant enzyme activities among diets, a general redox status was maintained in the cells. So while the colon was affected by changes in antioxidant enzyme levels, perhaps the mechanisms by which proliferation was inhibited in black sorghum rats and apoptosis was induced in brown sorghum rats were not ROS-dependent.

Our end phenotype, ACF, showed a significant sorghum effect in the ability to suppress colon carcinogenesis. The white sorghum rats, though not significantly different from cellulose, had a numerically lower amount of ACF when compared to cellulose. This numerical reduction could be attributed to the elevation of peroxidatic CAT activity in the quenching of H_2O_2 and the potential inhibition of CAT oxidase

activity. The black sorghum rats had fewer ACF than cellulose. This could be due to the synergistic effect of enhanced SOD activity and 3-deoxyanthocyanidins on the inhibition of proliferation via AP-1 suppression. Finally, the brown sorghum rats had fewer ACF than all other diets. These rats had the highest apoptotic index, potentially due to the condensed tannins, which have previously been shown to induce apoptosis in human colon cancer cell lines (70, 71). In addition to these observations, all sorghum diets suppressed GPx activity, displaying an ability of the exogenous antioxidant load to down-regulate need for endogenous antioxidant enzymes. This suggests that colonocytes from rats consuming sorghum bran were able to handle the oxidative injury at the time of the carcinogen injections, due in part to the high antioxidant activities of the diets.

CHAPTER VI

SUMMARY AND CONCLUSIONS

Summary. Sorghum had a significant effect on the suppression of colon carcinogenesis in rats as measured by a reduction in ACF being formed. The suppression of ACF in rats consuming varying types of sorghum occurred in part through their differential actions on endogenous antioxidant enzymes, proliferation, and apoptosis. White sorghum was effective at enhancing CAT activity while black sorghum enhanced SOD activity. All sorghum diets suppressed GPx activity. In addition, black sorghum effectively inhibited proliferation and brown sorghum enhanced apoptosis. These varying effects of sorghum diets on endogenous enzymes and cell cycle responses suggest that the different bioactive compounds present in the diets could be the causative agents. More research is needed to determine the specific effect of these compounds in their potential ability to suppress colon carcinogenesis.

Conclusions. Bioactive compounds that are present in sorghum have been previously shown to inhibit carcinogenesis (56, 68-73). Our findings also demonstrate the ability of sorghum bran to suppress colon carcinogenesis. Due to the differential actions of the sorghum brans on antioxidant enzymes and cell cycle responses, we believe that this suppression is in part due to the bioactive compounds present in the bran of these grains. These bioactive compounds could be functioning via mechanisms presented by other studies (**Fig. 31**). Future research with sorghum is merited in regards

to colon cancer prevention given that the specific mechanisms of action of these bioactive compounds in sorghum have yet to be identified. To sum up, sorghum has the capability to suppress colon carcinogenesis and the bioactive compounds in the grain should be considered further as potential chemoprotective agents.

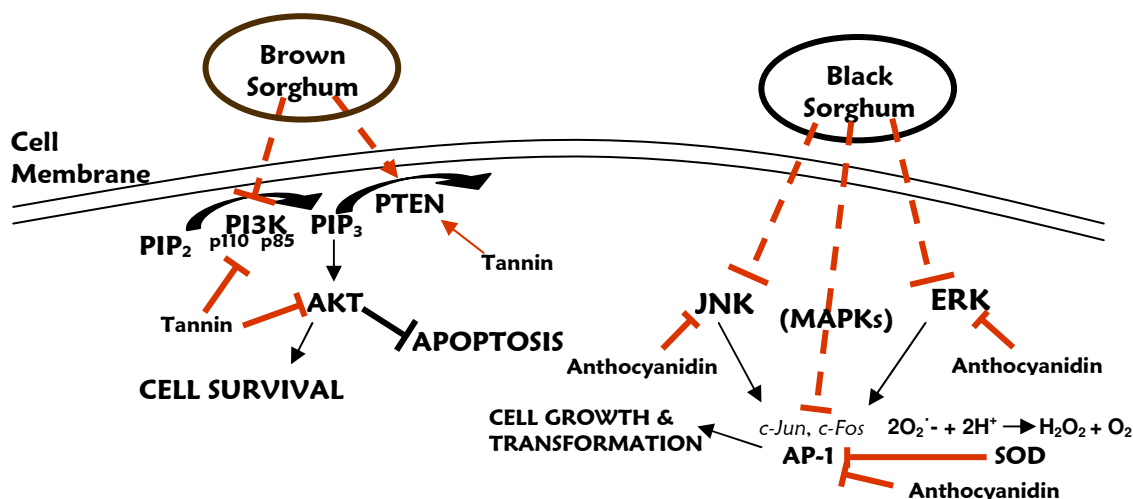


FIGURE 31 Potential Mechanisms Involved in Black and Brown Sorghum Effects. Engelbrecht (73) has shown the ability of condensed tannins to induce apoptosis via the reduction of both the catalytic (p110) and regulatory (p85) subunits of PI3K, suppressing its activity. PI3K phosphorylates PIP₂, generating PIP₃ which activates AKT, a promoter of cell survival. Condensed tannins were also able to attenuate activation of AKT. The condensed tannin was also able to decrease PTEN phosphorylation, making it more active as a negative regulator of the PI3K/AKT signaling pathway. Perhaps the condensed tannins present in brown sorghum diet were able to induce apoptosis through inhibition of PI3K through similar pathways as observed by Engelbrecht. Hou (69) has shown the ability of anthocyanidins to inhibit transcription factor, AP-1, an important transcription factor in proliferation that is inducible by tumor promoters. Anthocyanidins were also able to inhibit MAPKs c-Jun N-terminal kinase (JNK) and extracellular signal-regulated protein kinase (ERK). He postulated that this may be due to the ortho-dihydroxyphenyl structure on the B-ring of the anthocyanidins, a structure also present on luteolinidin, the main 3-deoxyanthocyanidin in black sorghum bran. Interestingly, he found a synergistic effect of anthocyanidins and SOD activity on the inactivation of AP-1. We also found increased SOD activity in black sorghum rats. Perhaps the suppression of proliferation was due to mechanisms similar to those described by Hou in which anthocyanidins are able to inhibit AP-1 activation in part to scavenging of superoxide radicals and in part to blocking MAPK pathways.

Future Research. This was a preliminary study designed to make general observations about the effects of sorghum brans, and possibly the compounds in the bran, on colon carcinogenesis. We saw significant effects of this grain in a colon cancer model, but further research is needed.

Future research is needed in order to study the mechanisms of action of our bioactive compounds of interest (luteolinidin, apigenidin, tannins). A study is needed to measure the activation of transcription factor AP-1 in response to 3-deoxyanthocyanidins present in sorghum, luteolinidin and apigenidin. It would also be beneficial to measure levels of tumor-suppressor gene p53 or anti-apoptotic PI3K levels in response to condensed tannins. Perhaps cell culture models should be employed first, followed by animal studies using diets supplemented with the compounds themselves.

It would also be beneficial to study actual uptake and bioavailability of these bioactive compounds in the colon. If the compounds are tightly bound to fiber, they could make it to the colon intact and have a direct effect on the luminal environment or the colonocytes themselves. Gu et al recently did an excellent job studying the uptake of sorghum phenols in female Sprague-Dawley rats (76). In the future, we should model this study with our actual compounds of interest in the diet to determine if they act alone, or if it is indeed a synergistic effect with the rest of the sorghum bran.

LITERATURE CITED

1. Landis S, Murray T, Bolden S, Wingo P. Cancer statistics, 1999. *CA Cancer J Clin.* 1999;49:8-31.
2. Heron MP, Smith BL. Deaths: Leading causes for 2003. *National Vital Statistics Reports.* 2007;55:1-93.
3. AICR. Food, nutrition, and the prevention of cancer: A global perspective. Washington, D.C.; 1997.
4. Martin KR. Targeting apoptosis with dietary bioactive agents. *Exp Biol Med.* 2006;231:117-29.
5. Jones JM. Grain-based foods and health. *Cereal Food World.* 2006;51:108-13.
6. Lupton JR. Is fiber protective against colon cancer? Where the research is leading us. *Nutrition.* 2000;16:558-61.
7. Rooney TK, Rooney LW, Lupton JR. Physiological characteristics of sorghum and millet brans in the rat model. *Cereal Food World.* 1992;37:782-6.
8. Schatzkin A, Mouw T, Park Y, Subar AF, Kipnis V, Hollenbeck A, Leitzmann MF, Thompson FE. Dietary fiber and whole-grain consumption in relation to colorectal cancer in the nih-aarp diet and health study. *Am J Clin Nutr.* 2007;85:1353-60.
9. Awika JM, Rooney LW. Sorghum phytochemicals and their potential impact on human health. *Phytochemistry.* 2004;65:1199-221.
10. Yang CS, Landau JM, Huang M-T, Newmark HL. Inhibition of carcinogenesis by dietary polyphenolic compounds. *Annu Rev Nutr.* 2001;21:381-406.
11. Bueso FJ, Waniska RD, Rooney WL, Bejosano FP. Activity of antifungal proteins against mold in sorghum caryopses in the field. *J Agric Food Chem.* 2000;48:810-6.

12. MacLean WC, Jr., Lopez de Romana G, Gastanaduy A, Graham GG. The effect of decortication and extrusion on the digestibility of sorghum by preschool children. *J Nutr.* 1983;113:2071-7.
13. Burkitt D. Epidemiology of cancer of the colon and rectum. *Cancer.* 1971;28:3-13.
14. Chen F, Cole P, Mi ZB, Xing LY. Corn and wheat-flour consumption and mortality from esophageal cancer in shanxi, china. *Int J Cancer.* 1993;53:902-6.
15. Van Rensburg SJ. Epidemiological and dietary evidence for a specific nutritional predisposition to esophageal cancer. *J Natl Cancer Inst.* 1981;67:243-51.
16. Bresalier RS. Chemoprevention of colorectal cancer: Why all the confusion? *Curr Opin Gastroenterol.* 2008;24:48-50.
17. Fodde R. The apc gene in colorectal cancer. *Eur J Cancer.* 2002;38:867-71.
18. Weinberg RA. Cancer: A genetic disorder. In: Mendelsohn J, Howley PM, Israel MA, Liotta LA, editors. *The molecular basis of cancer.* Philadelphia: W. B. Saunders; 2001. p. 3-9.
19. Fearon ER, Gruber SB. Molecular abnormalities in colon and rectal cancer. In: Mendelsohn J, Howley PM, Israel MA, Liotta LA, editors. *The molecular basis of cancer.* Philadelphia: W.B. Saunders; 2001. p. 289-312.
20. Pitot H, Hikita H, Sargent L, Haas M. Review article: The stages of gastrointestinal carcinogenesis- application of rodent models to human disease. *Aliment Pharmacol Ther.* 2000;14:153-60.
21. Das P, Jain D, Vaiphei K, Wig J. Abberant crypt foci – importance in colorectal carcinogenesis and expression of p53 and mdm2: A changing concept. *Dig Dis Sci.* 2008;53:2183-8.
22. Bird RP. Role of aberrant crypt foci in understanding the pathogenesis of colon cancer. *Cancer Lett.* 1995;93:55-71.

23. Pretlow TP, Barrow BB, Ashton WS, O'Riordan MA, Pretlow TG, Jurcisek JA, Stellato TA. Aberrant crypts: Putative preneoplastic foci in human colonic mucosa. *Cancer Res.* 1991;51:1564-7.
24. Pretlow TP, O'Riordan MA, Pretlow TG, Stellato TA. Aberrant crypts in human colonic mucosa: Putative preneoplastic lesion. *J Cell Biochem.* 1992;16G:55-62.
25. Roncucci L, Stamp D, Medline A, Cullen JB, Bruce WR. Identification and quantification of aberrant crypt foci and microadenomas in the human colon. *Hum Pathol.* 1991;22:287-94.
26. Pereira MA, Khoury MD. Prevention by chemopreventive agents of azoxymethane-induced foci of aberrant crypts in rat colon. *Cancer Lett.* 1991;61:27-33.
27. Bird RP, Good CK. The significance of aberrant crypt foci in understanding the pathogenesis of colon cancer. *Toxicol Lett.* 2000;112-113:395-402.
28. Vanamala J, Leonardi T, Patil BS, Taddeo SS, Murphy ME, Pike LM, Chapkin RS, Lupton JR, Turner ND. Suppression of colon carcinogenesis by bioactive compounds in grapefruit. *Carcinogenesis.* 2006;27:1257-65.
29. Magnuson BA, Shirliff NN, Bird RP. Resistance of aberrant crypt foci to apoptosis induced by azoxymethane in rats chronically fed cholic acid. *Carcinogenesis.* 1994;15:1459-62.
30. Shpitz B, Bomstein Y, Mekori Y, Cohen R, Kaufman Z, Grankin M, Bernheim J. Proliferating cell nuclear antigen as a marker of cell kinetics in aberrant crypt foci, hyperplastic polyps, adenomas, and adenocarcinomas of the human colon. *Am J Surg.* 1997;174:425-30.
31. Renehan AG, Booth C, Potten CS. What is apoptosis, and why is it important? *BMJ.* 2001;322:1536-8.
32. Sjoström J, Bergh J. How apoptosis is regulated, and what goes wrong in cancer. *BMJ.* 2001;322:1538-9.

33. Zornig M, Baum W, Hueber A-O, Evan G. Programmed cell death and senescence. In: Mendelsohn J, Howley PM, Israel MA, Liotta LA, editors. *The molecular basis of cancer*. Philadelphia: W. B. Saunders; 2001. p. 19-40.
34. Bedi A, Pasricha PJ, Akhtar AJ, Barber JP, Bedi GC, Giardiello FM, Zehnbauser BA, Hamilton SR, Jones RJ. Inhibition of apoptosis during development of colorectal cancer. *Cancer Res*. 1995;55:1811-6.
35. Cohen SM, Ellwein LB. Genetic errors, cell proliferation, and carcinogenesis. *Cancer Res*. 1991;51:6493-505.
36. Chang WC, Chapkin RS, Lupton JR. Predictive value of proliferation, differentiation and apoptosis as intermediate markers for colon tumorigenesis. *Carcinogenesis*. 1997;18:721-30.
37. Matés JM, Sánchez-Jiménez FM. Role of reactive oxygen species in apoptosis: Implications for cancer therapy. *Int J Biochem Cell Biol*. 2000;32:157-70.
38. Sanders LM, Henderson CE, Hong MY, Barhoumi R, Burghardt RC, Wang N, Spinka CM, Carroll RJ, Turner ND, et al. An increase in reactive oxygen species by dietary fish oil coupled with the attenuation of antioxidant defenses by dietary pectin enhances rat colonocyte apoptosis. *J Nutr*. 2004;134:3233-8.
39. Guyton KZ, Liu Y, Gorospe M, Xu Q, Holbrook NJ. Activation of mitogen-activated protein kinase by H₂O₂: Role in cell survival following oxidant injury. *J Biol Chem*. 1996;271:4138-42.
40. Manna SK, Zhang HJ, Yan T, Oberley LW, Aggarwal BB. Overexpression of manganese superoxide dismutase suppresses tumor necrosis factor-induced apoptosis and activation of nuclear transcription factor- κ B and activated protein-1. *J Biol Chem*. 1998;273:13245-54.
41. Musonda CA, Chipman JK. Quercetin inhibits hydrogen peroxide (H₂O₂)-induced κ B DNA binding activity and DNA damage in hepg2 cells. *Carcinogenesis*. 1998;19:1583-9.

42. Cadenas E, Davies KJA. Mitochondrial free radical generation, oxidative stress, and aging. *Free Radic Biol Med.* 2000;29:222-30.
43. Kannan K, Jain SK. Oxidative stress and apoptosis. *Pathophysiology.* 2000;7:153-63.
44. Rainis T, Maor I, Lanir A, Shnizer S, Lavy A. Enhanced oxidative stress and leucocyte activation in neoplastic tissues of the colon. *Dig Dis Sci.* 2007;52:526-30.
45. Matés JM, Pérez-Gómez C, De Castro IN. Antioxidant enzymes and human diseases. *Clin Biochem.* 1999;32:595-603.
46. Vives-Bauza C, Starkov A, Garcia-Arumi E. Measurements of the antioxidant enzyme activities of superoxide dismutase, catalase, and glutathione peroxidase. *Methods Cell Biol.* 2007;80:379-93.
47. Wu G, Fang Y-Z, Yang S, Lupton JR, Turner ND. Glutathione metabolism and its implications for health. *J Nutr.* 2004;134:489-92.
48. Salganik RI. The benefits and hazards of antioxidants: Controlling apoptosis and other protective mechanisms in cancer patients and the human population. *J Am Coll Nutr.* 2001;20:464S-72.
49. Adom KK, Sorrells ME, Liu RH. Phytochemical profiles and antioxidant activity of wheat varieties. *J Agric Food Chem.* 2003;51:7825-34.
50. Schober TJ, Bean SR, Boyle DL. Gluten-free sorghum bread improved by sourdough fermentation: Biochemical, rheological, and microstructural background *J Agric Food Chem.* 2007;55:5137-46.
51. Carr TP, Weller CL, Schlegel VL, Cuppett SL, Guderian DM, Jr., Johnson KR. Grain sorghum lipid extract reduces cholesterol absorption and plasma non-hdl cholesterol concentration in hamsters. *J Nutr.* 2005;135:2236-40.
52. Awika JM, McDonough CM, Rooney LW. Decorticating sorghum to concentrate healthy phytochemicals. *J Agric Food Chem.* 2005;53:6230-4.

53. Dykes L, Rooney LW. Phenolic compounds in cereal grains and their health benefits. *Cereal Food World*. 2007;52:105-11.
54. Grassi D, Lippi C, Necozione S, Desideri G, Ferri C. Short-term administration of dark chocolate is followed by a significant increase in insulin sensitivity and a decrease in blood pressure in healthy persons. *Am J Clin Nutr*. 2005;81:611-4.
55. Kurosawa T, Itoh F, Nozaki A, Nakano Y, Katsuda S-i, Osakabe N, Tsubone H, Kondo K, Itakura H. Suppressive effects of cacao liquor polyphenols (clp) on ldl oxidation and the development of atherosclerosis in kurosawa and kusanagi-hypercholesterolemic rabbits. *Atherosclerosis*. 2005;179:237-46.
56. Ramljak D, Romanczyk LJ, Metheny-Barlow LJ, Thompson N, Knezevic V, Galperin M, Ramesh A, Dickson RB. Pentameric procyanidin from theobroma cacao selectively inhibits growth of human breast cancer cells. *Mol Cancer Ther*. 2005;4:537-46.
57. Turner ND, Vanamala J, Leonardi T, Patil BS, Murphy ME, Wang N, Pike LM, Chapkin RS, Lupton JR. Grapefruit and its isolated bioactive compounds act as colon cancer chemoprotectants in rats. *Amer Chem Soc Abstract AGFD129*. Philadelphia, PA; 2004.
58. Awika JM, Rooney LW, Waniska RD. Properties of 3-deoxyanthocyanins from sorghum. *J Agric Food Chem*. 2004;52:4388-94.
59. Awika JM, Rooney LW, Waniska RD. Anthocyanins from black sorghum and their antioxidant properties. *Food Chem*. 2004;90:293-301.
60. Dykes L, Rooney LW. Sorghum and millet phenols and antioxidants. *J Cereal Sci*. 2006;44:236-51.
61. Roy HK, Gulizia JM, Karolski WJ, Ratashak A, Sorrell MF, Tuma D. Ethanol promotes intestinal tumorigenesis in the min mouse. *Cancer Epidemiol Biomarkers Prev*. 2002;11:1499-502.

62. Hong MY, Chapkin RS, Morris JS, Wang N, Carroll RJ, Turner ND, Change WCL, Davidson LA, Lupton JR. Anatomical site-specific response to DNA damage is related to later tumor development in the rat azoxymethane colon carcinogenesis model. *Carcinogenesis*. 2001;22:1831-5.
63. Marklund S. Distribution of cuzn superoxide dismutase and mn superoxide dismutase in human tissues and extracellular fluids. *Acta Physiol Scand Suppl*. 1980;492:19-23.
64. Mitaru BN, Reichert RD, Blair R. The binding of dietary protein by sorghum tannins in the digestive tract of pigs. *J Nutr*. 1984;114:1787-96.
65. Knudsen KEB, Kirleis AW, Eggum BO, Munck L. Carbohydrate composition and nutritional quality for rats of sorghum to prepared from decorticated white and whole grain red flour. *J Nutr*. 1988;118:588-97.
66. Jacobs LR, Lupton JR. Relationship between colonic luminal ph, cell proliferation and colon carcinogenesis in 1,2 dimethylhydrazine treated rats fed high fiber diets. *Cancer Res*. 1986;46:1727-34.
67. Lupton JR, Coder DM, Jacobs LR. Long-term effects of fermentable fibers on rat colonic ph and epithelial cell cycle. *J Nutr*. 1988;118:840-5.
68. Shih CH, Siu SO, Ng R, Wong E, Chiu LCM, Chu IK, Lo C. Quantitative analysis of anticancer 3-deoxyanthocyanidins in infected sorghum seedlings. *J Agric Food Chem*. 2007;55:254-9.
69. Hou D-X, Kai K, Li J-J, Lin S, Terahara N, Wakamatsu M, Fujii M, Young MR, Colburn N. Anthocyanidins inhibit activator protein 1 activity and cell transformation: Structure-activity relationship and molecular mechanisms. *Carcinogenesis*. 2004;25:29-36.
70. Gosse F, Guyot S, Roussi S, Lobstein A, Fischer B, Seiler N, Raul F. Chemopreventive properties of apple procyanidins on human colon cancer-derived metastatic sw620 cells and in a rat model of colon carcinogenesis. *Carcinogenesis*. 2005;26:1291-5.

71. Kim YJ, Park HJ, Yoon SH. Anticancer effects of oligomeric proanthocyanidins on human colorectal cancer cell line, HCT-116. *World J Gastroenterol.* 2005;11.
72. Al-Ayyoubi S, Gali-Muhtasib H. Differential apoptosis by gallotannin in human colon cancer cells with distinct p53 status. *Mol Carcinog.* 2007;46:176-86.
73. Engelbrecht AM, Mattheyse M, Ellis B, Loos B, Thomas M, Smith R, Peters S, Smith C, Myburgh K. Proanthocyanidin from grape seeds inactivates the pi3-kinase/pkb pathway and induces apoptosis in a colon cancer cell line. *Cancer Lett.* 2007;258:144-53.
74. Vetrano AM, Heck DE, Mariano TM, Mishin V, Laskin DL, Laskin JD. Characterization of the oxidase activity in mammalian catalase. *J Biol Chem.* 2005;280:35372-81.
75. Percy ME. Catalase: An old enzyme with a new role? *Can J Biochem Cell Biol.* 1984;62:1006-14.
76. Gu L, House SE, Rooney L, Prior RL. Sorghum bran in the diet dose dependently increased the excretion of catechins and microbial-derived phenolic acids in female rats. *J Agric Food Chem.* 2007;55:5326-34.

APPENDIX A

EXPERIMENTAL PROTOCOLS

Kill Day Set-up & Checklist

General

- Tape bench papers on lab benches and line with extra bench papers; replace bench papers as necessary.
- Put up instruction/reminder sheets and Rat Kill List at every station.
- Put out gloves of all sizes, boxes of Kim wipes, sufficient napkins, and sharpies at each station.
- Make sure liver Rnase-free utensils and supplies are properly “Zapped” the day before kill.
- Label timers, ACF tub covers, homogenization tubes and pestles
- Tape 2 - 3 biohazard bags on benches where needed
- Make solutions, ensure plenty of reserves; chill those that require chilling.
 - RNase-free & regular 1X PBS
 - 4% PFA
 - 50% & 70% EtOH
 - Heparin Soln.
- Complete rat's 48-hr diet intakes
- Move homogenization buffer from freezer to fridge
- Put up rat kill lists and instruction sheets
- Inform Aleta to prepare cages, covers and a cart for rats to be moved up to 2nd floor
- Tapes & Dispenser
- Assemble rat transport cages

Kill Station

- Check CO₂ tank, chamber, weights, cover cloth
- Black trash bags for rat bodies
- PBS in squirt bottle-RNase Free
- Surgical tools
 1. Straight scissors (black handle)
 2. Bent large scissors
 3. Forceps-(1) bent, (1) straight
 4. Small blunt tip scissors
- Extra bench papers
- Weigh dishes, 1 big, 1 medium, 2 small labeled with rat #
- Extra weigh dishes all sizes

- Rat packs
- Gauze – lots
- Ice bucket for PFA cubes
- 1 ml pipette with tips
- Instruction sheet
- Liquid Nitrogen Container
- Sharps Container
- Sharpie
- Gloves

ACF Station

- Big weigh dishes labeled with rat # (for holding colon)
- PBS in squirt bottle (1)
- 600mL glass beaker (1) covered w/foil
- Ice bucket (to hold PBS beaker) (1)
- 10cc syringe attached with RNase-free round-tip needle (4)
- Scapels & blades (4)
- Forceps (1 straight, 1 bent)
- Small blunt-tip scissors (1)
- Medium weigh boats for colon
- Labeled Whatman filter papers (in ziplock bag)
- ACF tupperwares and glass plates (2)
- Boat with 70% ethanol
- 70% EtOH
- “ART XLP 200”, P200 pipette (1)
- Biohazard bag
- Record sheet for any observations

Cassetting Station

- Ice tubs for holding small specimen cups (1)
- Labeled timers with rat # (8)
- Labeled big specimen cup with lid for holding cassettes fixed in 70% EtOH (1)
- Labeled cassettes with sponges (2/rat)
- Forceps (1 straight, 1 bent)
- Small scissors (1)
- 1X PBS in squirt bottle
- Labeled rat #, date and fixation small specimen cups with lids (wrap ones) for holding cassettes fixed in 4% PFA (8)

- Large weigh boats labeled with rat #
- Cold 4% PFA
- 70% EtOH
- Igloo coolers for holding ice (2)
- Record sheet for PFA fixation EtOH changes

Mucosal Scrapping and Homogenization Stations

- Ice buckets for storing homogenization buffer and eppetubes
- Homogenization buffer
- Denaturation Buffer
- 2ml RNase free eppetube /rat
- Ice box for holding glass
- Piggyback racks for holding eppetubes
- Square ice box for holding square glass plate
- Microscope slides
- Curved forcep (1)
- Water in squirt bottle (from bottled sterile water)
- 1X PBS in squirt bottle
- “ART XLP 200”, “ART 1000E”, and “10 Reach” pipette tips
- P1000 pipette (2), P200 pipette (1), and P10 pipette (1)
- Small specimen cups for rinsing (2)
- 2-mL homogenization tubes and pestles (labeled and in ziplock bags) 2/rat
- Pre-weighed tubes for GSH/GSSH
- Homogenization instruction sheet
- Balance
- Data sheet

Protein Isolation Station

- Centrifuge machine
- Timer labeled (4)
- 1cc Luer-Lok syringe with 27G 1¼ needle (8+)
- Sharps container
- Labeled 0.65mL
- 2 mL eppetubes for protein (2) (1 white to centrifuge, 1 yellow to transfer supernatant)
- Ice chest to hold eppetubes (2)
- Piggyback rack
- P200 and P1000 pipettes and pipette tips

- Calculator
- Instruction sheet
- Remarks record sheet and sharpie
- Gloves

Liver Station

- 3 ice buckets
- Zapped glass plate (4)
- 1.8 ml tubes (2/rat)
- Labeled RNA later bottle – 5 ml (1/rat)
- Chopping tools (4)
- Zapped scissors
- NaCl and heparin solution (300 ml/ rat)
- Beaker 250 ml (covered w/foil)
- 10 ml syringe(2) and needles (1/rat)
- Cryobags for extra liver (1/rat)
- Kimwipes
- Gloves
- Catch Tub for liver perfusion
- Tub of Soapy Water
- Large liquid nitrogen container
- Spatulas –Spoon shaped (2), Straight (2)
- Pen, Sharpie
- Ziplock bag
- Instruction Sheet

Blood Station

- 1 ice bucket next to centrifuge
- 0.6 and 0.3 ml heparin tube
- 1 ml cryotube
- Container for liquid N₂
- Rotator and ice in cold room
- Centrifuge at 4 °C
- Balance
- Syringe 2 ml/needle
- Pipette heparinated
- 3 Marma tubes
- 1 marma – Ac tube
- Balancing tubes for centrifuge
- Recording Sheet

- Sharpie Pen

Morning of Kill

1. Take protease inhibitor and protein buffer (previously aliquoted) out of freezer to thaw.
2. Scoop lots of ice and fill necessary tubs, boxes, and mug; store the remaining in ice igloos.
3. Take out heparin solution keep on ice
4. Remove denaturation solution from fridge; keep in ice.
5. Turn on both centrifuges at appropriate temp.
6. Add protease inhibitor to buffer and keep in ice.
7. Prepare and move rats from basement to kill station; keep food in cages.
8. Assemble specimen cups for cassetting – put in tub filled with ice, fill with ice-cold 4% PFA, store in ice chest.
9. Fill ACF tubs and EtOH fixation specimen cups with 70% EtOH.

After Kill

1. Store samples in appropriate place
2. Clean up
3. Autoclave biohazard trash and bring to dumpster
4. Bring rat bodies to freezer in basement diet mixing room
5. Wash tools and glassware; put to dry in oven
6. Solution changes

Aberrant Crypt Foci Enumeration Protocol

(Cindy Warren, 2001. Modifications by Kim Paulhill, 8/2007)

Supplies:

Methelyne blue in clear specimen cup
PBS in clear specimen cup
70% Ethanol in clear specimen cup
Rubber gloves
Long stem cotton swabs
Labeled tissue samples in clear specimen cups
Clear grid (with ½ cm squares)
ACF score sheets
Flash Drive
Paper towels
Clip board

Procedure:

1. Place all supplies in small cooler with waffle lab bench paper in the bottom of cooler in case of spillage.
2. In the microscope room, turn on the four switches and prepare to use the microscope (computer, scope, TV screen, grey box).
3. Stain the tissue by dipping in the methylene blue for 10-45 seconds. If too dark dip it back into 70% ethanol.
4. Place on plastic grid taped onto microscope stage, beneath lens, 10X magnification. Take care not to touch the lens.
5. Note rat ID number, length of colon, date, etc. on the score sheet.
6. Starting on the distal end (this end doesn't have tissue architecture with ridges). Go slowly through each box, examining the tissue.
7. Note any ACF, both position and multiplicity.
 - i. Normal crypts are oval or round and a lighter blue stain.
 - ii. ACF are darker and have swirl-like appearance.
 - iii. Many of the ACF have increased size, thicker epithelial lining, and darker staining luminal openings.
 - iv. Compare the ACF to the surrounding tissue.
 - v. Hyperproliferative crypts are not as distorted as the ACF.
 - vi. ACF have a larger white, distorted zone in the luminal opening.
 - vii. Peyer's patches are lymphatic tissue; look like big cloudy spots.

8. Make sure that tissue does not dry out—using cotton swap, moisten tissue periodically with PBS. It should remain shiny.

Buffer Selection- Protein Homogenization

Three rats were killed to practice antioxidant assay in colon mucosa. Two different kinds of buffers were used to homogenize the protein: Dr. Wu's modified buffer and a modified version of that buffer. The buffer was modified by Jairam, Laurie and Dr. Turner, so the samples can be used for Western blot assays. Dr. Wu's modified buffer seemed to offer better results for antioxidant enzyme quantification than the modified homogenization buffer. Apparently the protein recovery is also higher with Dr. Wu's modified buffer. However, this buffer was used for the actual experiment. 10 mL of buffer were prepared for each killing day (8 rats).

Dr. Wu's Homogenization Buffer

1. Preparation of Stock solutions

Stock 1. 50mM K_2HPO_4 : Dissolve 4.35g of K_2HPO_4 in 500ml of deionized H_2O

Stock 2. 50mM KH_2PO_4 : Dissolve 3.4g of KH_2PO_4 in 500ml of deionized H_2O (use 1L bottle)

Stock 3. Prepare 50mM Potassium Phosphate buffer (pH 7.2)
Add 50mM K_2HPO_4 (stock 1) to 50mM KH_2PO_4 (stock 2) until pH is 7.2

Stock 4. Prepare 250mM Sucrose/1mM EDTA solution by dissolving 42.8g of sucrose and 186mg of disodium EDTA in 500ml of potassium phosphate buffer (stock 3). pH again to 7.2 (use KOH or HCl)

2. Preparation of homogenization buffer (adapted from Dr. Wu's assay for enzyme extraction). 250mM sucrose/1mM EDTA/1mM DTT in 50mM potassium phosphate buffer:

5ml	250mM sucrose/1mM EDTA solution (stock 4)
200 μ l	protease inhibitor cocktail
5 μ l	Triton X-100 (0.1%)
5 μ l	1M DTT solution (made fresh)
0.3858 mg	DTT in 2.5mL Phosphate Buffer

Dr. Wu's Modified Homogenization Buffer
(Modification suggested by Jairam, Laurie and Dr. Turner)

250 mM sucrose/1mM EDTA/1mM DTT in 50 mM potassium phosphate buffer. Modification consists of final concentration of 0.1% triton rather than 0.0001% and use of sodium orthovanadate.

Preparation of Dr. Wu's Modified Homogenization Buffer

1. Preparation of Stock solutions

Stock 1. 50mM K₂HPO₄: Dissolve 4.35g of K₂HPO₄ in 500ml of deionized H₂O

Stock 2. 50mM KH₂PO₄: Dissolve 3.4g of KH₂PO₄ in 500ml of deionized H₂O (use 1L bottle)

Stock 3. Prepare 50mM Potassium Phosphate buffer (pH 7.2)
Add 50mM K₂HPO₄ (stock 1) to 50mM KH₂PO₄ (stock 2) until pH is 7.2

Stock 4. Prepare 250mM Sucrose/1mM EDTA solution by dissolving 42.8g of sucrose and 186mg of disodium EDTA in 500ml of potassium phosphate buffer (stock 3). pH again to 7.2 (use KOH or HCl)

2. Preparation of homogenization buffer

Stock Solutions	10 mL Buffer	50 mL Buffer	Company cat. #	Storage
250 mM Sucrose/ 1mM EDTA solution (stock 4)	9.4 mL	47 mL	K ₂ HPO ₄ & KH ₂ PO ₄ (Sigma) Sucrose (Sigma S7903) EDTA (disodium) Sigma ED4SS	Frozen
Triton X-100 10%	100 µl	500 µl	Peroxidase free Calbiochem 648464	Frozen
1M DTT	10 µl	50 µl	Sigma D9779	Made fresh
10 mM Sodium orthovanadate	100 µl	500 µl	Sigma S6508	Frozen
Protease inhibitor	400 µl	2 mL	Sigma P8340	Add just before use

Coomassie Protein Assay

Equipment:

Microtiter plate reader (A595)

Reagents:

Coomassie Plus Protein Assay Kit Pierce 23236

- contains Coomassie Blue stain
- BSA standards (2mg/ml)

Procedure:

1. Prepare BSA standards:
 $2\mu\text{g}/\mu\text{l}$ (in kit)
 $500\mu\text{l}$ of $2\mu\text{g}/\mu\text{l}$ + $500\mu\text{l}$ ddH₂O = $1\mu\text{g}/\mu\text{l}$
 $125\mu\text{l}$ of $2\mu\text{g}/\mu\text{l}$ + $875\mu\text{l}$ ddH₂O = $0.25\mu\text{g}/\mu\text{l}$
 (this is sufficient for only one set of standards)
2. Prepare microcentrifuge tubes of standards and samples **in triplicate**. (Add Coomassie to all tubes last.)

Standards:

μg protein	$0.25\mu\text{g}/\mu\text{l}$ BSA	$1\mu\text{g}/\mu\text{l}$ BSA	$2\mu\text{g}/\mu\text{l}$ BSA	Water	Homog. Buffer	Coomassie Reagent
0	$0\mu\text{l}$	-	-	$498.75\mu\text{l}$	$1.25\mu\text{l}$	$500\mu\text{l}$
1	$4\mu\text{l}$	-	-	$494.75\mu\text{l}$		
2	-	$2\mu\text{l}$	-	$496.75\mu\text{l}$		
4	-	$4\mu\text{l}$	-	$494.75\mu\text{l}$		
10	-	$10\mu\text{l}$	-	$488.75\mu\text{l}$		
20	-	-	$10\mu\text{l}$	$488.75\mu\text{l}$	↓	↓

Samples:

Amt. of sample	Water	Coomassie Reagent
$1.25\mu\text{l}$	$498.75\mu\text{l}$	$500\mu\text{l}$

3. Incubate samples in Coomassie at RT for 10 minutes.
4. Transfer $300\mu\text{l}$ of each tube to the appropriate well on a microtiter plate.
5. Read absorbance (A595) on microtiter plate reader.
 (Absorbances for standards generally range from 0.3 to 1.0.)
6. Plot standard curve (absorbance vs. μg protein). Most plate readers will do this for you.
7. Use readout of “unknowns” to determine protein concentration of samples.

Superoxide Dismutase Assay

Cayman Chemicals

Catalog #706002

Range of Kit is 0.025-0.25 units/ml SOD

Contents of Kit

1. Assay Buffer (10X)
2. Sample Buffer (10X)
3. Radical Detector
4. SOD (standard)
5. Xanthine Oxidase
6. 96 Well Plate
7. Plate Cover

Additional Items Required

1. Potassium Cyanide (*needed for measuring mitochondrial SOD*)
2. Plate Reader with 450nm filter
3. Adjustable pipettors and a repeat pipettor
4. Glass distilled water or HPLC-grade water

Pre-Assay Preparation

1. Assay Buffer-(10X)-(Vial #1)
 - a. Dilute 3 ml of Assay Buffer with 27 ml of HPLC-grade water
Assay buffer is used to dilute Radical Detector
 - Store at 4°C-Stable for 2 Months
2. Sample Buffer-(10X)-(Vial #2)
 - a. Dilute 3 ml of Sample Buffer concentrate with 27 ml of HPLC-grade water
 - b. Final Sample Buffer should be used to prepare the SOD standards and dilute xanthine oxidase and SOD samples prior to assaying
 - Store at 4°C-Stable for 2 Months
3. Radical Detector-(Vial #3)
 - a. Put 19.95 ml of diluted Assay Buffer in a vial.
 - b. Transfer 50 µl of tetrazolium salt to vial, but not until right before you are about to add to wells.
 - c. Cover with Foil (light sensitive)
 - Stable for 2 hours on ice
4. SOD standard-(Vial #4)
 - a. Bovine Erythrocyte SOD(Cu/Zn)
 - i. Ready to use as supplied
 - ii. Store thawed enzyme on ice

5. Xanthine Oxidase (Vial #5)
 - a. Thaw one vial
 - i. Do not refreeze thawed enzyme
 - b. Transfer 50 μl of enzyme to another vial
 - c. Dilute with 1.95 ml of *diluted* Sample Buffer
 - Stable for 1 hour on ice

Performing the SOD Assay

- i. *The Assay temp is 25 C and absorbance is at 450 nm.*
- ii. *All reagents except samples and xanthine oxidase must be equilibrated to room temperature before beginning the assay.*

1. Preparation of SOD Standards:

- a. Dilute 20 μl of SOD standard (vial #4) with 1.98 ml of diluted Sample buffer to each tube as described below:
- b.

Tube	SOD Stock (μl)	Sample Buffer (μl)	Final SOD Activity (U/ml)
A*	0	1,000	0
B	20	980	0.025
C	40	960	0.05
D	80	920	0.1
E	120	880	0.15
F	160	840	0.2
G	200	800	0.25

* just add 10 μl of Sample Buffer to Standard A wells instead of making a tube

2. SOD Standard Wells

- a. Add 200 μl of diluted Radical Detector and 10 μl of Standard (tubes A-G) in designated wells on plate.
- b. For blanks, just add 210 μl of HPLC-graded water to well.

3. Sample Wells

- a. Add 200 μl of diluted Radical Detector and 10 μl of sample (in ratio desired).
- OR
- b. Add 190 μl of diluted Radical Detector, 10 μl of inhibitor (KCN), & 10 μl of sample.

4. Initiate the reaction by adding 20 μl of diluted xanthine oxidase to all wells.

- a. Note precise time when started.
- b. Add as quickly as possible

5. Shake plate for 5 seconds to mix and cover with plate cover.
6. Incubate on a shaker for 20 min at room temperature.
7. Read absorbance at 450 nm using a plate reader.

Calculating Results of SOD Assay

1. Calculate average absorbance of each standard and sample
2. Divide Standard A's absorbance by itself and divide standard A's absorbance by all the other standards and samples absorbances to yield the linearized rate (LR)
 - a. (*i.e.* $LR \text{ for Std A} = \text{Abs Std A} / \text{Abs Std. A}$; $LR \text{ for Std B} = \text{Abs Std A} / \text{Abs Std B}$)
3. Plot the linearized SOD standard rate (LR) as a function of final SOD Activity (U/ml) from Table 4. Calculate the SOD activity of the samples using the equation obtained from the linear regression of the standard curve substituting the linearized rate (LR) for each sample.
 - b. One unit is defined as the amount of enzyme needed to exhibit 50% dismutation of superoxide radical.
 - c. $\text{SOD(U/ml)} = [(\text{Sample LR} - \text{y-intercept}) / \text{slope}] \times (0.23\text{ml} / 0.01\text{ml}) \times \text{sample dilution}$

Catalase Assay Kit
Calbiochem # 219265

Materials Provided:

10X Assay Buffer
10X Sample Buffer
Formaldehyde Standard Kit
Catalase Control
Potassium Hydroxide
Methanol
Hydrogen Peroxide
Purpald
Potassium Periodate
96 Well Plate and Plate Sealer

Materials Required but not Provided:

Plate Reader (540 nm filter)
Adjustable Pipettor
Repeat Pipettor
Distilled or HPLC-grade water

Reagent Preparation

1. 10X Assay Buffer
 - a. Dilute 2ml 10X Assay Buffer with 18ml of HPLC-grade water
 - b. This is 1X Assay Buffer to be used in Assay
 - c. Store at 4°C-Stable for at least 2 months
2. 10X Sample Buffer
 - a. Dilute 5 ml of 10X Sample Buffer with 45 ml HPLC-grade water
 - b. This is 1X Sample Buffer should be used to dilute standards, controls, samples prior to assaying
 - c. Store at 4°C-Stable for at least 2 months
3. Catalase (Control)
 - a. Add 2 ml of 1X Sample Buffer and Vortex well
 - b. Take 100 μ l of reconstituted enzyme and dilute with 1.9ml of 1X Sample Buffer
 - c. Diluted enzyme is stable for 30 min
 - d. Reconstituted CAT is stable for one month at -20°C
4. Potassium Hydroxide
 - a. Place vial on ice, add 4ml cold HPLC-grade water and vortex
 - b. Store at 4°C stable for at least 3 months
5. Hydrogen peroxide
 - a. Dilute 40 μ l Hydrogen Peroxide with 9.96 ml HPLC-grade water
 - b. Dilute Hydrogen Peroxide solution is stable for 2h.

Performing the CAT Assay:

- 1) Prepare Formaldehyde Standards
 - a) Dilute 10 μ l of Formaldehyde Standard with 9.99 ml 1X Sample Buffer
 - b) Add the amount of Formaldehyde Standard and 1X Sample Buffer to each tube as laid out below

Tube	Formaldehyde Stock (μ l)	Sample Buffer (μ l)	Final Concentration (μ M formaldehyde)
A	0	1000	0
B	10	990	5
C	30	970	15
D	60	940	30
E	90	910	45
F	120	880	60
G	150	850	75

- 2) Formaldehyde Standard Wells
 - a) Add 100 μ l 1X Assay Buffer
 - b) 30 μ l Methanol
 - c) 20 μ l Formaldehyde Standards (tubes A-G)
- 3) Positive Control
 - a) Add 100 μ l 1X Assay Buffer
 - b) Add 30 μ l Methanol
 - c) Add 20 μ l diluted Catalase Control
- 4) Sample Wells
 - a) Add 100 μ l 1X Assay Buffer
 - b) Add 30 μ l Methanol
 - c) Add 20 μ l sample
- 5) Initiate the reactions by adding 20 μ l dilute Hydrogen Peroxide to all wells.

- a) Note time Started
- 6) Cover Plate with plate sealer and incubate on shaker for 20 min at room temp.
- 7) Add 30 μ l Potassium Hydroxide to each well to terminate reaction.
- 8) Add 30 μ l of Purpald to each well.
- 9) Cover plate with plate sealer and incubate for 10 min at room temp. on shaker.
- 10) Add 10 μ l Potassium Periodate to each well. Cover with plate sealer and incubate at room temp. on shaker for 5 min.
- 11) Read absorbance at 540nm.

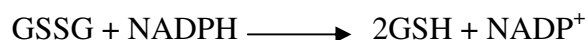
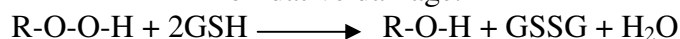
Calculating Results of Catalase Assay

- 1) Calculate avg. absorbance for each standard or sample
- 2) Subtract avg. absorbance of standard A from itself and all other standards and samples.
- 3) Plot corrected absorbance of standards as a function of final formaldehyde concentration
- 4) Calculate the formaldehyde concentration of the samples using the equation obtained from the linear regression of the standard curve substituting corrected absorbance values for each sample
 - a. Formaldehyde (μM) = (Sample absorbance - y-intercept / slope) x (0.17 ml / 0.02 ml)
- 5) Calculate Catalase Activity of the Sample using the following equation
 - a. One unit is defined as the amount of enzyme that will cause the formation of 1.0 nmol formaldehyde per min at 25°C
 - b. CAT Activity = (μM of sample / 20 min) x Sample dilution = nmol/min/ml

Glutathione Peroxidase Assay Protocol

Calbiochem: Cat. #353919

Glutathione peroxidase (GPx) catalyzes the reduction of hydroperoxides, including hydrogen peroxide, by reduced glutathione and functions to protect the cell from oxidative damage.



Contents of Kit

1. Assay Buffer (10x)
2. Sample Buffer (10x)
3. Glutathione Peroxidase (Control)
4. Co-Substrate Mixture (3 vials)
5. Cumene Hydroperoxide
6. 96 Well Plate & Plate Cover

Additional Items Required:

1. Plate reader
2. Adjustable pipettors & repeat pipettor
3. Glass distilled or HPLC-grade water

Reagent Preparation:

1. Assay Buffer (10x)
 - a. Dilute 2 ml Assay Buffer concentrate with 18 ml HPLC-grade water.
 - b. Used in the assay.
 - c. Store at 4°C. Stable for 2 months.
2. Sample Buffer (10x)
 - a. Dilute 2 ml Sample Buffer concentrate with 18 ml HPLC-grade water.
 - b. Used to dilute GPx Control and Samples prior to assaying.
 - c. Store at 4°C. Stable for 2 months.
3. Glutathione Peroxidase (Control)
 - a. To avoid repeated freezing and thawing, this should be put into small aliquots and stored at -20°C.
 - b. For assay, dilute 10 µl of the GPx Control with 490 µl of dilute Sample Buffer and keep on ice.
 - c. Stable for 4 hours on ice.
 - d. A 20 µl aliquot of diluted GPx per well causes a decrease of ~ 0.051 absorbance unit/minute.

4. Co-Substrate Mixture
 - a. Add 2 ml of HPLC-grade water to vial and vortex well.
 - b. Each reconstituted vial will be enough reagent for 40 wells.
 - c. The reconstituted reagent should be kept at 25°C while assaying.
 - d. Store at 4°C. Stable for 2 days.

5. Cumene Hydroperoxide
 - a. Ready to use as supplied.
 - b. Store at -20°C.

Performing the GPx Assay:

- The assay temperature is 25°C. Prepare all wells in triplicate.
1. Background Wells
 - a. Add 120 μ l dilute Assay Buffer.
 - b. Add 50 μ l Co-Substrate Mixture.
 2. Positive Control Wells
 - a. Add 100 μ l dilute Assay Buffer.
 - b. Add 50 μ l Co-Substrate Mixture.
 - c. Add 20 μ l dilute GPx Control.
 3. Sample Wells
 - a. Add 100 μ l dilute Assay Buffer.
 - b. Add 50 μ l Co-Substrate Mixture.
 - c. Add 20 μ l sample.
 4. Initiate the reaction by adding 20 μ l Cumene Hydroperoxide to all the wells.
 - a. Note precise time when started.
 - b. Add as quickly as possible.
 5. Carefully shake the plate for a few seconds to mix.
 6. Read the absorbance once every minute at 340 nm.
 - a. Obtain at least 5 time points.

Calculating Results of Glutathione Peroxidase Assay

1. Determine the change in absorbance (ΔA_{340}) per minute by:
 - a. Plotting the absorbance values as a function of time to obtain the slope.

-OR-

- b. Select two points on the linear portion of the curve and determine the change in absorbance during that time using the following equation:

$$\Delta A_{340}/\text{min} = \frac{A_{340}(\text{Time 2}) - A_{340}(\text{Time 1})}{\text{Time 2 (min)} - \text{Time 1 (min)}}$$

2. Determine the rate of $\Delta A_{340}/\text{min}$. for the background or non-enzymatic wells and subtract this rate from that of the sample wells. Use the following formula to calculate the Glutathione peroxidase activity. The reaction rate at 340 nm can be determined using the NADPH extinction coefficient of $0.00373 \mu\text{M}^{-1}$. One unit is defined as the amount of enzyme that will cause the oxidation of 1.0 nmol of NADPH to NADP^+ /min at 25°C .

$$\text{GPx Activity} = \frac{\Delta A_{340}/\text{min}}{0.00373 \mu\text{M}^{-1}} \times \frac{0.19\text{ml}}{0.02\text{ml}} \times \text{Sample dilution} = \text{nmol/min/ml}$$

HPLC Analysis of GSH, GSSG, Cystine and Cystine

Modified By Kim Paulhill 7/2007

The principle: the reduced form of glutathione (GSH) and the oxidized form of glutathione (GSSG), as well as cystine and cysteine, are derivatized with dansyl chloride in the presence of iodoacetic acid and KOH/tetraborate (pH 9.0) to yield fluorescence derivatives. The derivatives are separated by HPLC and quantified using fluorescence detection.

1. Chemicals:

- a. Sodium Heparin
- b. Bathophenanthroline Disulfonate Sodium Salt (BPDS)
- c. Iodoacetic Acid
- d. Dansyl Chloride
- e. L-serine
- f. GSH
- g. GSSG
- h. Cystine
- i. Cysteine
- j. Sodium Acetate Trihydrate
- k. Boric Acid
- l. Sodium Tetra Borate

2. Preparation of Solvents and Reagents:

- a. 100 mM Boric Acid: Dissolve 3.1g boric acid in 500ml HPLC H₂O
- b. 100 mM Sodium Tetraborate: Dissolve 19.1g sodium tetraborate in 500ml HPLC H₂O

i. Solution A (Preservation Solution):

1. Dissolve 1.05g L-Serine
2. 50 mg sodium Heparin
3. 100 mg BPDS
4. 200 mg iodoacetic acid
5. in 80 ml of 100mM boric acid
6. 20 ml of 100mM sodium tetraborate
7. Solution is stable at -80°C for 6 months
8. *(Note: Heparin to inhibit coagulation, serine-borate to inhibit degradation of GSH by (-glutamyltranspeptidase, bathophenanthroline disulfonate to inhibit GSH oxidation, and iodoacetic acid to alkylate GSH).*

ii. Solution B (10% perchloric acid, w/v; 0.2 M boric acid):

1. Dissolve 6.2 g boric acid in 300 ml HPLC water
2. Add 71 ml of 70% perchloric acid
3. quiesce to 500ml with HPLC water

iii. Derivatization solutions:

1. KOH/tetrahydroborate solution (pH 9.0):
 - a. Add 5.6 g KOH
 - b. to a plastic bottle containing 50g $K_2B_4O_7 \cdot 4H_2O$ and 100ml HPLC water
 - c. Mix- (*Stable indefinitely at 25°C*)
2. Iodoacetic Acid:
 - a. Dissolve 14.8 mg iodoacetic acid in 2ml of HPLC water
 - b. *Made fresh the day of derivatization*
3. Dansyl chloride:
 - a. Dissolve 200mg dansyl chloride in 10ml of HPLC acetone
 - b. *Made fresh the day of derivatization*

3. GSH, GSSG, Cystine, and Cysteine standards:

- a. 2 mM GSH, GSSG, Cys, and Cystine:
 - i. Dissolve 6.16 mg GSH
 - ii. 12.2 mg GSSG
 - iii. 2.44 mg cysteine
 - iv. 4.8 mg cystine
 - v. In 5ml of Sol A + 5ml of Solution B
- b. 500 nmol/ml GSH, GSSG, Cys, and Cystine:
 - i. Mix 50 μ l of 2 mM standards
 - ii. With 75 μ l of Sol A+ 75 μ l of Sol B
- c. 50 nmol/ml GSH, GSSG, Cys, and Cystine:
 - i. Mix 50 μ l of 2 mM standards
 - ii. With 975 μ l of Sol A+ 975 μ l of Sol B
- d. Blank (0 nmol/ml):
 - i. Mix 200 μ l of Sol A+ 200 μ l of Sol B

4. Extraction of Glutathione from Tissue

- a. Tissue Homogenization for small sample size;(~ 5 to 10 mg tissue)
 - i. Homogenize the tissue in 0.1 ml Sol A+ 0.1 ml Sol B
 - ii. Rinse Homogenizer with 0.1 ml Sol A + 0.1 ml Sol B
 - iii. Combine Homogenates
 - iv. Centrifuge all tubes at 10,000 g for 1 min.
 - v. Use supernatant for derivatization

5. Derivatization

- a. Add to 1.5 ml microcentrifuge tube (use amber tubes):
 - i. 150 μ l of standards (0, 50, 500 nmol/ml) or samples
 - ii. 30 μ l of Iodoacetic acid solution
 - iii. 100 μ l of KOH/tetraborate sol. (pH ~9)
 - iv. Vortex and wait 20 min
- b. Add 150 μ l of dansyl chloride solution to each tube
 - i. Vortex

- ii. Keep all tubes in dark at room temp. for 16 h.
- c. Add 250µl of HPLC-grade chloroform to each tube(to extract the free dansyl-Cl)
 - i. Vortex and centrifuge at 10,000 g for 1 min
 - ii. (*The dansyl derivatives are stable in the dark at 0-4°C for 12 months*)
 - iii. Use upper aqueous layer for HPLC analysis
- d. Add 100µl of sample (or standard) derivatives to a micro-insert tube in a brown vial
 - i. Vortex
 - ii. Injection volume: 25µl

6. HPLC Analysis

- a. HPLC solvents:
 - i. Solvent A (Acetic Acid Buffer, pH 4.6)
 - 1. 640 ml Methanol + 200 ml Acetate stock solution +125 ml Glacial acetic acid + 50 ml HPLC water
 - 2. (*Acetate Stock solution: Dissolve 272 g sodium acetate trihydrate in 122 ml HPLC water and 378 ml glacial acetic acid*)
 - ii. Solvent B (80% Methanol; v/v):
 - 1. 800 ml HPLC Methanol + 200 ml HPLC water
- b. HPLC Column: 3-Aminopropyl column (5 µm; 4.6 x 250 mm)
 - i. Custom LC, Houston, TX: Tel 800-537-9339)

- c. HPLC solvent gradient:

Solvent	Time(min)					
	0	10	30	33	33.1	38
Solvent A (%)	20	20	80	80	20	20
Solvent B (%)	80	80	20	20	80	80

Flow rate: 1.0 ml/min

Fluorescence detection (Waters 2475 Multi λ Fluorescence Detector):

0.0 to 7.5 min: 590 nm excitation; 610 nm emission

7.5 to 38 min: 335 nm excitation; 610 nm emission

Gain: 10 (0 to 32.2 min): 100 (32.2 to 38 min).

- (For liver samples)

Gain: 100 (0 to 32.2 min): 1000 (32.2 to 38 min).

- (For other samples)

Attenuation: 1

Retention time: Cys-16.7 min, Cysteine-20.1 min, GSH- 29.4 min, GSSG- 38 Min

Chemicals & supplies needed:

Name	Supplier & Catalog #
Sodium Heparin	Sigma H4784
Bathophenanthroline disulfonate sodium salt (BPDS)	Sigma B1375
Iodoacetic acid	Sigma I2512
Dansyl chloride	Sigma 39220 (Fluka)
L-serine	Sigma S4500
GSH standard	Sigma G6529
GSSG standard	Sigma G6654
Cystiene Standard	Sigma C-7352
Cystine Standard	Sigma C122009
Sodium acetate trihydrate	Sigma 236500
Boric acid	Sigma B0394
Sodium tetraborate	Sigma 221732
70% Perchloric acid	Fisher A469
HPLC grade water	Fisher W7
Potassium hydroxide (KOH)	Sigma P5958
Potassium tetraborate tetrahydrate	Sigma P5754
Acetone	Fisher A949
Chloroform	Sigma 650498
Glacial acetic acid	Bio/Bio
Methanol (HPLC grade)	Fisher A452
3-aminopropyl column	CEL Associates #132-204 Ph# 800-537-9339 Pearland, TX

Other supplies & equipment needed:

balance	tweezers
1.5 ml eppi tubes (2/sample)	ice & ice chest
vortex	mini vortexer
mini centrifuge	HPLC glass vials with springs, inserts & lids
pipet and tips	calculator
HPLC insert tubes	Waters Wat72030

PCNA methodology

Staining protocol using the sequenza slide rack (Shandon, Pittsburgh, PA)

Reagents:

1. Phosphate buffered saline (PBS)
2. Vectastain ABC Elite Kit -- mouse IgG
source: Vector Lab.
Cat #: PK-6102, 1 ml/ea.
contains: blocking serum
biotinylated antimouse IgG
avidin-biotin complex
3. PCNA monoclonal antibody (anti-PC10, murine)
source: Signet lab
Cat #: 523-01, 1ml/ea
ps. Each new lot # of anti-PC10 must be tested with a 1:50, 1:100, 1:150, 1:200 dilution series. Prepare antibody dilution with PBS, under sterile conditions. Use 4 micro thick single serial sections of colonic tissue to test the antibody dilutions. Record the optimal dilution for the lot # tested.
4. Diaminobenzidine or DAB-tetrahydrochloride
source: Sigma
Cat #: D-5637
 - Prepare DAB stock solution, 50 mg/ml in H₂O. Store as 2 ml aliquots at -20° C.
5. Harris hematoxylin

Critical steps prior to staining:

1. tissue fixation in 70% ethanol.
2. processing and baking of tissue at temperatures not exceeding 50° C.
3. keep slides moist at all times during the staining procedure.
4. include one positive and one negative control slide in each batch of slides stained.

Performing the PCNA Assay:

1. Deparaffinize slides

xylene-----5' x 3
 100% EtOH-----5' x 2
 95% EtOH-----3' x 2
 70% EtOH-----3'
 H₂O -----3'

2. Leave slides in 3% H₂O₂ for 30 min to remove endogenous peroxidase activity.

3% H₂O₂: 20 ml of 30% H₂O₂ made up to a final volume of 200 ml with methanol.

3. Wash in PBS 5 min, 3 times.

Mount slides onto coverplates using PBS and insert into sequenza.

4. Prepare Vectastain Blocking Serum by adding 3 drops of stock Normal Serum (yellow label) to 10 ml of PBS in yellow mixing bottle.

5. Add 3 drops* to each coverplate in sequenza and replace top to maintain humidity. Let stand for 20 min.

6. Wash with PBS by filling each coverplate in the sequenza with one ml of PBS.

7. Add 150 µl of anti-PC10 (use the optimal dilution obtained by dilution series: 1:200) to each coverplate in sequenza and replace top. For the negative control slide use PBS instead of anti-PC10. Let stand for 1 hour.

8. Wash with PBS by filling each coverplate in the sequenza to the top with PBS. Let stand for 5 min.

9. Prepare Vectastain biotinylated anti-mouse IgG by mixing 3 drops of stock normal serum with 10 ml PBS in Blue mixing bottle, then add 1 drop of stock biotinylated antibody (blue labe), Mix Gently. (or use 5 ml of serum solution form step 4, mix with 25 µl of stock biotinylated antibody)

10. Add 3 drops to each coverplate in sequenza and replace top. Let stand for 45 min.

11. Prepare ABC reagent in advance to be used in step 13. The ABC reagent is prepared by adding 2 drops of reagent A (gray label) to 5 ml PBS in the ABC Reagent large mixing bottle. Then add exactly 2 drops of Reagent B (gray label) to the same mixing bottle, mix immediately, and allow ABC Reagent to stand for about 30 minutes before use. This should be done in a darkened area.

* Note: 1 drop = 50 μ l

12. Wash with PBS by filling each coverplate in the sequenza to the top with PBS. Let stand for 5 min.

13. Apply Vectastain ABC reagent that had been prepared in step 11. Add 3 drops to each coverplate in sequenza, replace top, and let stand for 30 min.

14. Wash with PBS by filling each coverplate in the sequenza to the top with PBS. Remove slides from sequenza and place in PBS for 5 min.

15. Prepare DAB solution

For 200 ml: 2 ml stock DAB (50 mg/ml)

bring volume up to 200 ml with PBS

Immediately before staining, add 100 :l 30% H₂O₂.

16. Leave slides in DAB solution for 1 min, agitate twice.

17. Wash with H₂O 5 min, 3 times.

18. Deactivate all DAB materials (glassware, pipet tips, used stock vials, stir bars) and used DAB solutions with bleach overnight, and flush with excess water in drain next day.

19. Counterstain with Hematoxyline \leq 1 sec.

20. Wash with H₂O 2 min, 2 times.

21. Dehydrate slides:

1 x 1 min 70% ETOH.

1 x 1 min 95% ETOH.

1 x 1 min 100% ETOH.

1 x 2 min Xylene.

22. Apply permount and cover glass. Use the wet mounting method.

Apoptosis – ApopTag

Modified by Lisa Sanders for NSBRI initiation study

Used by Jayme Lewis for Sorghum Project

Original Protocol: ApopTag Kit with modifications by Wen-Chi Chang & April Carney

02/2006

Note: To be performed on 4%PFA fixed tissue.

***Put 200 ml PBS for Prot. K in 37° C oven and begin bleach rinse.

- ___ 1. Deparaffinize and rehydrate tissue:
 - ___ Xylene, 3X, 5 min
 - let xylene just dry, circle sections w/ PAP pen, dry 1 min
 - ___ 100% EtOH, 2X, 5 min
 - ___ 95% EtOH, 1X, 3 min
 - ___ 70% EtOH, 1X, 3 min
 - ___ PBS, 1X, 5 min

(Get Equilibration Buffer and Reaction Buffer out of freezer-put on ice)
- ___ 2. Pretreat tissue – 3 min, in 37°
Proteinase K (10 µg/ml PBS) = 0.1 ml Proteinase K (Ambion # 2546) in
200 ml PBS.
- ___ 3. Wash in dH₂O, 2x, 2 min
- ___ 4. Quench Endogenous Peroxidase: 0.3% H₂O₂ in 100% Methanol:
3.0 ml 30% H₂O₂ in 297 ml 100% Methanol or 2.0 ml in 198 ml(add fresh H₂O₂
immediately before quenching). 30 min, RT
- ___ 5. Wash in dH₂O, 2x, 5 min
- ___ 6. Wash all slides in PBS 5 min.
- ___ 7. Gently tap off PBS and carefully blot around sections. (Do this step and
following step one slide at a time to avoid drying out sections.)
- ___ 8. Apply EQUILIBRATION BUFFER to all sections: incubate in humidified
chamber for 15 sec to 1 hr @ RT.
(# of slides X 150 µl) (9 slides X 150µl = 1.35 ml)

- ___9. Tap off equilibration buffer and immediately apply REACTION BUFFER (-controls) or working strength TdT Enzyme with dilution ratio 1/10 (enzyme /reaction buffer). (Get TdT directly from freezer & keep on ice)

Apply only reaction buffer to – control sections:

___(# sections) X 40µl

For normal sample sections (# sections X 40µl):

___1080 µl reaction buffer (for 9 slides)

___36 µl TdT enzyme (for 9 slides)

Incubate in a humidified chamber at 37°C, 1 hr
(Prepare Stop/Wash so it can warm to RT.)

- ___12. Put slides in coplin jar with Working Strength Stop/Wash Buffer (1ml + 34 ml dH₂O). Agitate for 15 sec; incubate 10 min, RT.
Take aliquot of ANTI-DIGOXIGENIN PEROXIDASE (# slides X 125 µl) and allow to warm to room temperature (9 slides x 125µl = 1.125ml)
- ___14. Wash slides in PBS, 3X, 1min
- ___15. Blot dry the slides quickly (do one slide at a time) and apply ANTI-DIGOXIGENIN PEROXIDASE to all sections; incubate 30 min. in humidity chamber @ RT.
- ___16. Wash in PBS 4X, 2min
Prepare DAB peroxidase (1:50, substrate:dilution buffer) (#slides x 150µl) and warm to room temperature. Protect from light. (9 slides X 150µl = 1350µl = 27µl substrate:1323µl dilution buffer)
- ___17. Blot dry the slides quickly (do one slide at a time) and stain sections with DAB until light brown color shows up (≤ 1 min).
- ___18. Wash in dH₂O, 3X, 1 min
Leave in 4th for 5 min
- ___19. Counterstain w/ Methyl Green (reusable):
Dip quickly into Methyl green
Rinse in dH₂O 5X; dip 1x in the 1st 2 changes and briefly agitate
Dip 10 x in 3rd & leave ~ 30 sec.

Leave in the last 2 for 1 min w/o agitation

___20. Dehydrate: ALL FRESH

___70% EtOH, 1X, 1 min

___95% EtOH, 1X, 1 min

___100% EtOH, 1X, 1 min

___Xylene: 3X, 2 min (dip 10 times/ea)

___21. Wet mount w/ Permount (80:20, Permount:Xylene) – leave overnight to dry

reagent	company	catalog #
Apotag Kit:	Chemicon	S7101
Proteinase K	Ambion	2546
PBS	Life Technologies	21600-069

APPENDIX B
DATA TABLES

TABLE 5
Weight Gain Data¹

Diet	Weight Gain		
	Wk 2	Wk 7	Wk 10
	<i>g/24 h</i>		
Cellulose	5.766 ± 0.323 ^a	2.886 ± 0.433 ^{a,b}	1.891 ± 0.459 ^a
White Sorghum	6.168 ± 0.323 ^a	3.438 ± 0.433 ^a	1.767 ± 0.459 ^a
Black Sorghum	6.312 ± 0.323 ^a	1.894 ± 0.433 ^b	1.036 ± 0.459 ^a
Brown Sorghum	6.323 ± 0.323 ^a	2.885 ± 0.433 ^{a,b}	1.070 ± 0.459 ^a

¹Average weight gain data of rats over 48 hr time period at wk 2, 7, and 10. Data are means ± SEM for n=10 rats/diet. Means without common letter differ (p < 0.02).

TABLE 6
Feed Efficiency Data¹

Diet	Feed Efficiency		
	Wk 2	Wk 7	Wk 10
Cellulose	0.350 ± 0.016 ^a	0.157 ± 0.021 ^{a,b}	0.107 ± 0.027 ^a
White Sorghum	0.369 ± 0.016 ^a	0.177 ± 0.021 ^a	0.098 ± 0.027 ^a
Black Sorghum	0.391 ± 0.016 ^a	0.111 ± 0.021 ^b	0.063 ± 0.027 ^a
Brown Sorghum	0.374 ± 0.016 ^a	0.163 ± 0.021 ^{a,b}	0.058 ± 0.027 ^a

¹Feed efficiency data of rats at three different time points. Data are means ± SEM for n=10 rats/diet. Means without common letter differ (p < 0.03).

TABLE 7
Crypt Height¹

Diet	Crypt Height <i># cells/crypt</i>
Cellulose	31.93 ± 0.495 ^a
White Sorghum	32.24 ± 0.495 ^{a,b}
Black Sorghum	32.35 ± 0.495 ^{a,b}
Brown Sorghum	33.36 ± 0.495 ^b

¹Total number of cells/crypt. Data are means ± SEM for n=10 rats/diet. Means without common letter differ (p < 0.05).

TABLE 8
Total Number of Light Stained Cells in Proliferation¹

Diet	Light Stained Cells in Proliferation <i># cells/crypt</i>
Cellulose	3.092 ± 0.380 ^a
White Sorghum	2.812 ± 0.380 ^a
Black Sorghum	2.784 ± 0.380 ^a
Brown Sorghum	3.500 ± 0.380 ^a

¹Total number of light stained cells/crypt. Data are means ± SEM for n=10 rats/diet. No means differ.

TABLE 9
Total Number of Stained Cells in Proliferation¹

Diet	Light Stained Cells in Proliferation <i># cells/crypt</i>
Cellulose	7.500 ± 0.819 ^a
White Sorghum	6.052 ± 0.819 ^a
Black Sorghum	5.280 ± 0.819 ^a
Brown Sorghum	6.928 ± 0.819 ^a

¹Total number of stained cells/crypt. Data are means ± SEM for n=10 rats/diet. No means differ.

TABLE 10
Total Proliferative Index¹

Diet	Total Proliferative Index <i># cells/crypt height</i>
Cellulose	23.89 ± 2.497 ^a
White Sorghum	19.56 ± 2.497 ^a
Black Sorghum	17.15 ± 2.497 ^a
Brown Sorghum	21.31 ± 2.497 ^a

¹Total number of stained cells (light and dark combined)/total number of cells in crypt. Data are means ± SEM for n=10 rats/diet. No means differ.

TABLE 11
Apoptotic Index of Bottom Tertile¹

Diet	Apoptotic Index in Bottom Tertile
	<i># cells/crypt height</i>
Cellulose	2.538 ± 0.735 ^a
White Sorghum	2.108 ± 0.735 ^a
Black Sorghum	2.727 ± 0.735 ^a
Brown Sorghum	3.564 ± 0.735 ^a

¹Apoptotic cells/total number of cells in crypt in bottom tertile. Data are means ± SEM for n=10 rats/diet. No means differ.

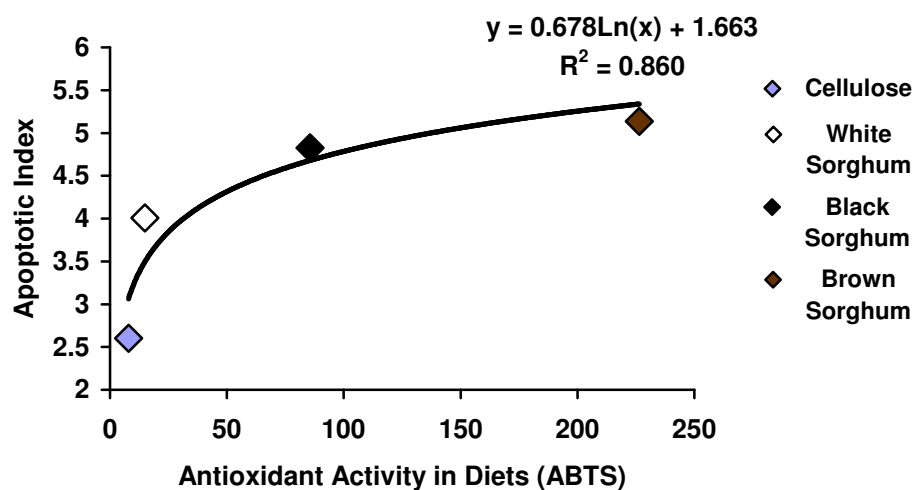


FIGURE 32 Apoptotic Index vs. Antioxidant Activity. Four experimental diets were fed to 40 AOM-injected rats (n=10/diet). The antioxidant activity of the diets was measured by 2,2'-azino-bis(3-ethylbenzthiazoline-6-sulphonic acid (ABTS) method. Apoptotic index was calculated from the distal colon of all animals with the TUNEL assay. There was a tendency for apoptotic index to increase as antioxidant activity in the diet increased ($p < 0.07$).

VITA**JAYME BETH LEWIS****Permanent Address:**

Texas A&M University
2253 TAMU
College Station, Texas 77843

Education:

Texas A&M University, College Station, TX
M.S. in Nutrition, December 2008, GPA: 4.0

Texas A&M University, College Station,
B.S. in Nutritional Sciences, May 2006, GPA: 3.96

Awards:

Honorary Mention, Student Poster Competition, April 2008
ASN Diet and Cancer Research Section, Experimental Biology

Third Place, Student Poster Competition, March 2008
Intercollegiate Faculty of Nutrition Symposium, TAMU

Poster Presentation, November 2007
Prevention of Cancer Meeting, AICR

Academic Scholarship, May 2007 & May 2008
Intercollegiate Faculty of Nutrition, TAMU

Regents Graduate Fellowship, September 2006- August 2007
Intercollegiate Faculty of Nutrition, TAMU

Outstanding Senior Award for Nutritional Sciences, May 2006
Gamma Sigma Delta, TAMU

Publications:

Lewis JB, Taddeo SS, McDonough CM, Rooney LW, Carroll RJ, Turner ND. Sorghum bran varieties differentially influence endogenous antioxidant enzymes to protect against oxidative stress during colon carcinogenesis. *FASEB J.* 2008; 22:887.7.

Memberships:

American Society for Nutrition
American Dietetic Association
Texas Dietetic Association
Cambridge Who's Who